Modified serpentine motion of the snake robot

A thesis

submitted in fulfilment

of the requirements for the degree

of

Master of Engineering

at

The University of Waikato

by

Pinwei Jin

THE UNIVERSITY OF
WAIKATO
Te Whare Wānanga o Waikato

University of Waikato

2015

Abstract

The frequent occurrence of earthquake in New Zealand drives the research on snake robot for search and rescue operation because of its elongated body shape and locomotion mimicry of the biological snake. Both features are in favour of moving the snake robot through the earthquake disaster area. To facilitate the robot control and information gathering, it is usually required to install a camera on the snake robot head so that the video images of the disaster area can be send back to the human operator. This thesis presents the simulation of a snake robot performing serpentine motion. A camera is attached on the snake robot head to obtain the video image along the line of sight. A remote controller is incorporated to control the advancement based on the video images. This simulation reveals that the video images from the camera oscillate seriously because the camera on the snake robot head follows serpenoid curve during the locomotion. As a result, both robot control and information gathering are affected. A solution is proposed to stabilize the snake robot head and its camera by introducing a correction at the joint between the robot head and its body. This correction aligns the camera sight direction with the moving direction of the snake robot to yield satisfactory video images. Finally, an actual snake robot is implemented with a wireless camera installed on the head to show the effect of correction. Experiments are conducted to control the advancement of snake robot remotely just based on the video images obtained from the camera. This greatly improves the performance of the snake robot.

Keywords: snake robot, simulation, serpentine motion, head modification, remote control

Acknowledgements

I would like to acknowledge and thank the many people who have contributed to this thesis. My supervisor, Dr. Chi Kit Au, for his patience, guidance and assistance during the research and preparation of the thesis.

I would like to add a special thank to Natalie Guest who helped to work on the media release for my project, to Mary Dalbeth and Dr. James Carson for offering me a lot of help in registration and thesis submission.

At last I would like to thank my parents and my family for their support during my study at Waikato University in New Zealand.

Contents

List of Figures

List of Table

Chapter 1. Introduction

New Zealand is a country being a part of Pacific Ring of Fire is geologically active. About 2000 earthquakes occur every year, most of them are minor, but still about 200 of these are strong enough to be felt. Some big earthquakes leaded to serious damages including house destroying, diseases and death (Wikipedia, 2014).

Figure 1.1 Destroyed buildings in 2011 Christchurch earthquake (Healthy Being, 2014).

The most recently big earthquake happened in Christchurch caused widespread damage, especially in the central city and eastern suburbs, with damage exacerbated by buildings and infrastructure already being weakened by the 4 September 2010 earthquake and its aftershocks. Significant liquefaction affected the eastern suburbs, producing around 400,000 tonnes of silt. In total, 185 people were killed in the earthquake, making it the second-deadliest natural disaster recorded in New Zealand (after the 1931 Hawke's Bay earthquake), and fourth-deadliest disaster of any kind recorded in New Zealand, with nationals from more than 20 countries among the victims. Over half of the deaths occurred in the six-storey Canterbury Television Building, which collapsed and caught fire in the quake. The total cost to insurers of rebuilding was originally estimated at NZ$15 billion. At that point it was already predicted to be by far New Zealand's costliest natural disaster and the third-costliest earthquake worldwide. But by April 2013, the total estimated cost had ballooned to $40 billion. Some economists have estimated it will take the New Zealand economy 50 to 100 years to completely recover (Wikipedia, 2014).

1.1 Motivation

Compared with the economic lose, value of life is worthless. Therefore, search and rescue operations after the earthquake are important. Hundreds of lives will be saved if search and rescue operations are conducted efficiently and effectively. However, there are many restrictions to delay the rescue operations due to the complicated situations caused by earthquake. For instance, lack of detecting devices to find the alive trapped people, the inefficient approach to deliver the

emergency goods to sufferers are two common examples. Besides, the unnecessary injury occurred to rescue stuff during aftershocks is another major issue to consider.

In the disastrous event of the NY World Trade Centre in 2001, robots for searching victims were dispatched and performed rescue operation. This is the first incident of search and rescue operation performed by rescue robots and has shown the usefulness of robotic technology in large-scale disasters (J. Casper, 2002). In such a large-scale disaster, the complicated particular environments disturbed the rescue robot mobility. Hence, mobility and size are the two major criteria for selecting a robot for the search and rescue operation.

Snakes are able to move on various environments. They can adapt to a particular terrain employing changes in their muscles-shape (Kane and Lecision, 2000). This yields the attempts of approaching biological inspired snake locomotion in the robot mobility during the search and rescue operations. Snake robots accomplish their locomotion by means of body motions. Compared with the wheeled, tracked and legged robots, snake robot can move across uneven terrain since it is not dependent on wheels and tracks. It can also move across soft ground such as sand as it distributes its weight across a wider area that legged robot. Furthermore, the relatively smaller cross section and large movement volume make a snake robot can be send into the destroyed buildings and dangerous places to gather the environmental information for the rescue planning. In addition, a snake robot can transport the emergency medicine and clear water to the trapped people for the

first-aid appliance. Figure 1.2 shows some ideas of using the snake robot for various rescue operations.

Figure 1.2 Snake robots act as an assistant for rescue and dangerous tasks (ROBONOR, 2014).

Although employing the snake robots for the search and rescue operations has received much attention in the past few years, most of the researchers are still remaining in the areas of locomotion such as kinematics and dynamics of the system. In order to apply the snake robot to the disastrous environment, both theoretical and practical significance are important. Therefore, it is necessary to implement and demonstrate its utility on the search and rescue operation so that more issues such as sensing robot control and operation can be explored.

1.2 Objectives and scopes

The objective of the research is to investigate the feasibility of employing a snake robot for visual environmental information gathering in a search operation. Due to the advantage of biological snake locomotion on various terrain, most of the snake (or snake inspired) robotics search concentrate in the kinematics, dynamics and locomotion control. All these works are developed based on the robot itself, various sensors such as vision and temperature detection systems are not equipped with the robot. However, the effectiveness of these sensing systems is highly dependent upon the locomotion of the robot. As a result, this research will investigate if there are any significant issues of using of a wireless camera to gather the visual environment information with emphasis on the underlying principles of snake inspired locomotion.

The scopes of the search include three major respects:

1. Snake robot mobility

   There are at least five types of biological snake locomotion: lateral undulation, side winding, concertina, rectilinear and slide-pushing. The lateral undulation is the most popular locomotion in the snake robotics research community. Hence, the snake robot used in this research will mainly concentrate on the lateral undulation locomotion.

2. Robot control

A tele-operated snake robot will be used in this research project because the presence of humans in the control loop is considered as the ultimate and safe solution, Furthermore, tele-operation systems are the only ones putting in close and constrained contact robots and humans. In fact, employing a tele-operated snake robot in the search yields a simple human-machine interaction and reduces the complexity of the snake robot design so that the feasibility study can be pin-pointed on the visual environmental information gathering. However, a snake robot, that performs behaviours or tasks with a high degree of autonomy, is desirable in the search and rescue operation eventually.

3. Environmental information gathering

Environmental information is important in the search and rescue operation. Not only for the tele-operator to control the snake robot movement, has it also provided information for planning the rescue operation. A wireless camera is equipped with a snake robot to gather the visual information which is transmitted to the tele-operator for further processing.

1.3 Methodology

Both simulation and implementation will be performed to explore the issue of using a snake robot equipped with a wireless camera for rescue operation. The methodology is listed:

1. A snake robot is designed based on the off-the shelf components such as brackets, servo motors and micro controller by using CAD software Solidworks.

2. The geometric model of the snake robot is then transferred into the robotics software V-REP for simulation.

3. The mathematical principle of the serpentine motion, which is the simulation of the snake lateral undulation, is studied. Based on the serpentine curve and kinematics of the robot, a control algorithm for the servo motors is derived in the software V-REP to simulate the locomotion of the snake robot model. A vision system is attached to the head of snake robot to obtain the video image. Based on the video image, an operator controls the snake robot movement in the simulation environment.

4. A snake robot prototype is then implemented. A wireless camera is installed on the head of snake robot as the vision system. A gamepad module and receiver are also attached to the snake so that the tele-operator can send the instruction to the snake robot and control its motion based on

the video images transmitted from the wireless camera (at the head of the snake robot).

5. Investigation will be performed to check if there is any major issue in the process.

Chapter 2. Literature review

Snake robots are a series of hyper-redundant chained mechanisms consisting of kinematical constrained links. The many degrees of freedom make them difficult to control but provide potential locomotion skills in cluttered and irregular environments, which are similar to the environmental situations after earthquake. Inspired by the robustness and stability of biological snake locomotion, this robotic mechanism designed to move like a biological snake and typically consist of many serially connected joint modules capable of bending in one or more planes which enable them to move on irregular surface. Snake robots carry the potential of meeting the growing need for robotic mobility in unknown and challenging environments (Liljebäck, Pål, 2012).

As a potential research project, snake robots have gained a lot of attentions since early days in 1970s. With the improvement of technology on sensors and manufacturing, snake robots were developed in generations. The following paragraphs give a brief introduction about four main aspects of snake robot, which are locomotion, snake robot control, implementation and the application.

2.1 Locomotion of snake robot

Many kinds of approaches have been proposed to locomote the snake robot. The most common snake robot locomotion is lateral undulation. Other movements like sidewinding and rolling also be employed on snake robot.

2.1.1 Lateral undulation

When it comes to snake robot, the most remarkable researcher in early years is Professor Hirose. He developed the Active Chord Mechanism (ACM) series snake robots and utilized the serpentine motion. Professor Hirose was inspired by the biological snake and developed the equation of serpenoid curve, which has now become a mainstay on the bookshelves of many researchers, presents an excellent overview of the research he has conducted over the years (Hirose, 1993).

Lateral undulation is implemented as a sine-like wave propagating down the body of the snake robot from the head to the tail. It can be divided into two categories: ones where passive wheels are applied, such as the Hirose's snake robot; ones where wheels are not added. An alternative description of lateral undulation, named the serpentine curve, was proposed by Ma, where a mathematical model of the muscle characteristics of snakes is employed to derive the resulting form of the body shape during lateral undulation. Ma concluded that snake locomotion according to the serpentine curve has a higher locomotive efficiency than locomotion according to the serpenoid curve. The locomotive efficiency during slip-free motion was defined as the ratio between the tangential and normal direction friction forces on the snake body (Ma, 2001).

For the undulation motion without wheels, Bayraktaroglu and Blazevic adopt an approach in their own version of a wheel-less snake robot by utilizing push-points created by pegs to provide the propulsive force while undergoing a modified form of lateral undulation. The push-points in the initial research are activated by linear actuators at both end of the link, while in later prototypes, the push-points need no longer be actuated, as sensors are used to find the suitable push-points and adjust the joint angles accordingly (Bayraktaroglu et al., 2006).

2.2.2 Side winding

Side winding is the most common gait that the snake adapts in the desert. when moving, the snake rear part of body will stick to ground first, the head part will move to the front aside. After the head part reaches ground, the rear moves in the same direction.

Burdick and his colleagues researched this motion and deduced the equation and implement using hyper-redundant snake robot in several situations, like the uniform direction side winding in flat surface and turning motions during movement. They focused on continuous morphology mechanisms, and also showed by way of example hat a discrete mechanical structure to implement this gait. The conclusion they got is that the side winding locomotion is most useful for fast gross displacement (Burdick et al., 1993).

2.2.3 Other approaches to locomotion

Some other locomotion like Sinus-lifting has been studied and implemented by Ma. They used a 2D model which took advantage of the contact force with ground as the propulsion. It also shows that the snake moves forward faster using Sinus-lifting than using lateral undulation (Ma & Inoue, 2004).

Lateral rolling is another common snake robot locomotion, Ohno and Hirose discussed it in their research. They employed the SR module to assistant them to accomplished these locomotion. SR module is the pneumatic module with three degrees of freedom, and has pneumatic actuators, valves, displacement sensors, springs and a microprocessor inside its body. The Slim Slime Robot they made consisted of several SR modules, and the following figure shows the lateral rolling motion (Ohno & Hirose, 2001).

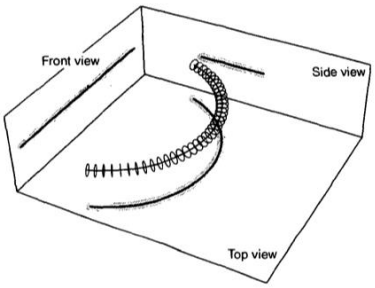

Figure 2.1 Lateral rolling

2.2 Snake robot control

It is difficult to control a snake robot effectively due to the fact that snake robots have high degrees of freedom. Most of the snake robots have a complicated model with various calculations or with very little environmental adaptability. There are three most common approaches in the snake robots research field, which are based on the trajectory, torque and central pattern generator (CPG).

In trajectory-based control, a trajectory of snake robot is proposed first, then the angular variables such as angular velocity and angular acceleration of every segment is deduced based on the trajectory curve. Together with the kinematics model and dynamics model, the actuator torque of each joint is calculated. The serpenoid motion (Hirose, 1993) employs this method. Meanwhile, a trajectory tracking control law for the wheeled snake robot was derived by Fumitoshi and Hiroki (Fumitoshi & Hiroki, 2005). In the trajectory control, a problem of singular configuration such as having all segments aligned in a line should be avoided. A control law to avoid this singular configuration was discussed by Fumitoshi and Hiroki(Fumitoshi & Hiroki, 2005).

Torque based control refers to the control of the torque in joints directly in order to realize the locomotion. It is similar to how a biological snake controls its movement. However, this control strategy is difficult to achieve in the snake robot. The reason is that the snakes have the ability to precisely control the forces of their muscles, whereas in robots the precise control of actuator torques is often a challenge. David Rollinson and his colleagues (Rollinson et la., 2014) designed a controller that adapted to the terrain solely by controlling joint torques, without explicitly sensing the contacts between the robot and the environment. They

implemented a Series Elastic Actuated Snake robot (SEA Snake shown in figure 2.2) which consisted a series of modules with actuators. This approach enables sensitive and stable torque control at each joint, while the high torque capabilities of geared motors are maintained.

Figure 2.2 SEA snake robot which enables the torque sensing

The last kind of control approach is based on the central pattern generator (CPG).This is a bio-inspired locomotion control method in robots and become popular these days. Animals are controlled by this kind of rhythm generating mechanism (Mattiaet et la., 2004). In Williamson's theory (Williamson, 1998), the CPG can generate the self-deduced oscillation even without a high command control. This advantage results the popularity of using the CPG in the robots control. CPG is a neural network which generates the parameters for an actuator. In the research by Ma and Wu (Ma & Wu, 2010) presented a new network with feedback connection and investigated the relation characteristics between the CPG parameters and the outputs. Desired locomotion patterns can be achieved by adjusting the CPG parameters correspondingly from the results.

Two modes are employed to implement the control approach. The first one is centralized control, which means that the master module computes and makes decisions according to the overall situations, then dispatches the movement of other modules uniformly. In another word, the master controller calculates the joint angles of every motor due to the motion planning and distributes the joint angle to the motors. It is easy to realize because it concentrates the control functions. Another control approach distributes the control mode. The master controller only manages the joint variable parameters and sent out these parameters to the executive module. The executive modules then calculate the joint angles of their own modules.

Although the centralised control mode is easy to realize, it brings to much workload to the master module. Hence, a local failure will cause the mistakes in the whole system. Meanwhile, the distributed control mode has higher system reliability and stability and it has a relatively more complicated control structure (Wang et la., 2003).

2.3 Implementation

2.3.1 ACM robots

The world first snake robot was designed and implemented by Professor Shigeo Hirose from Tokyo Institute of technology in 1976. It is called ACM-III, which means Active Cord Mechanism. Another contribution Professor Hirose made was he deduced the formulation of the serpenoid curve, which is the way how the biological snake moves. The ACM-III is 2 meters long and contains 20 joints, just like biological snakes' articulations. It can move parallel to the ground and the maximum speed can be 40centimetres per second. There are two passive wheels under each joint, these wheels reduce the frictional coefficient between the robot body and ground and avoid slip during moving. Therefore, the snake robot can get the enough propulsion to move forward when crawling. The ACM-III can only move in one dimension and its body cannot leave the ground surface.

This project was laid aside for quite a long period of time, and after almost 2 decades in 1997 Professor Hirose and his colleagues modified their snake robot with a new generation called ACM-R1. Unlike the ACM-III, ACM-R1 had a less 16 modules and a faster speed which could reach 50 centimetres per second. Another thing to highlight is that this prototype had wireless device on both snake and controller, it broke the limit come from the cables, which made the snake move within controlling in long-distance.

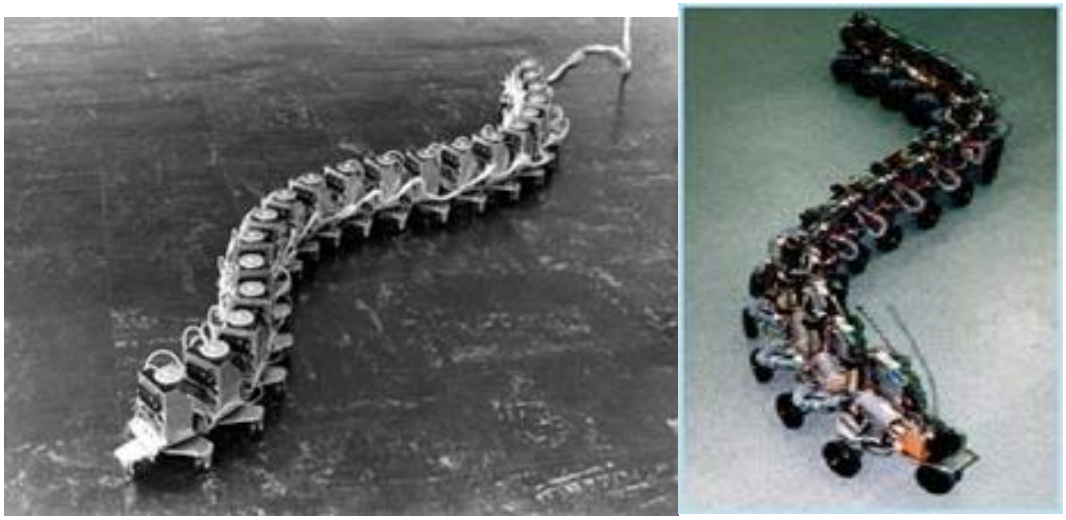

Figure 2.3 ACM-III (left) and ACM-R1 (right)

Three years later, the following ACM-R2 came out with a 3 dimensional prototype. This snake allowed each joint to rotate in horizontal and vertical plane. And in 2000, they optimized it with ACM-R3, which had the same function with the former one. Each module had one degree of freedom with compacter structure and lighter mass. “This ACM-R3 is equipped with large passive wheels which wrap its overall body, and has frictional characteristic as snake-like skin. It is also equipped with radio controlled servomotors with some gears added to them, and held tightly by shell flames so that it can move steadily and with high power” (Mori et al., 2001).

Figure 2.4 ACM-R2 (up) and ACM-R3 (down)

In order to improve its suitability, they developed ACM-R4 with some big breakthroughs. The degrees of freedom are 18 and weight is 9.5 kilograms. Compared with ACM-R3, it only has 9 modules and the following merits. (1)Active wheels: ACM-R4 has motors to drive wheels. In general, snake-like robots can generate propulsive force by undulating their body and don't need motors for wheels. However, the movement requires large number of joints, so active wheels are adopted from the viewpoint of practical use of snake-like robots; (2) Dust and water-proofing: ACM-R4 adopts shell structure and is equipped with rubber seals at the joints and wheel shafts, which enable continuous 3-hours operation in muddy water; (3) Overload Protection: To protect robot from a shock and overload expected in practical use, over load protection is implemented.

ACM-R4 has a simple clutch using O-ring. The friction force of O-ring transmits the torque from an internal gear to the joint (H. Yamada & S. Hirose, 2006).

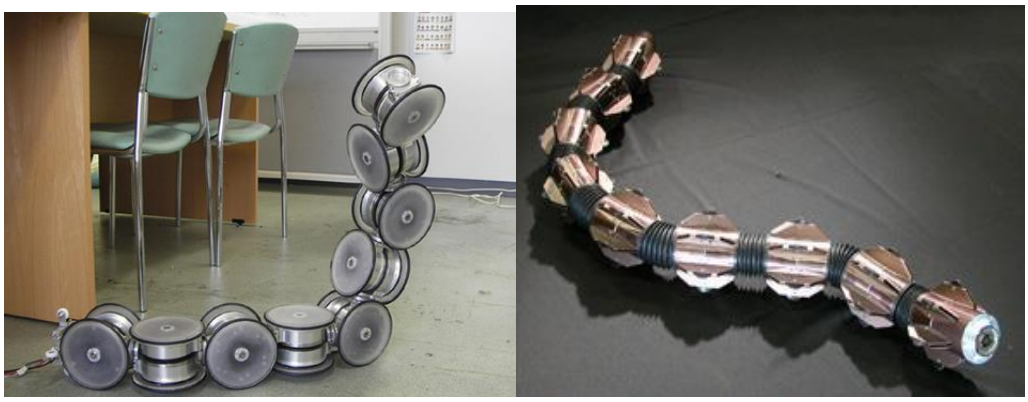

Figure 2.5 ACM-R4 and ACM-R5

The latest ACM snake robot is ACM-R5, as the figure 2.5 shows. It is a perfect assembly with 9 modules developed on the basis of model HELIX. The joints of ACM-R5 are universal joints which allow it moves in an effective locomotion. To be precise, the universal joint has one passive twist joint at the intersection point of two bending axis to prevent mechanical interference with bellows. ACM-R5 is equipped with paddles and passive wheels around the body. To generate propulsive force by undulation, the robot need a resistance property as it glides freely in tangential direction but cannot in normal direction. Due to the paddles and passive wheels, ACM-R5 obtains that character both in water and on ground.

2.3.2 CMU's robot

The snake robot from Carnegie Mellon University is developed by Biorobotics Lab research group directed by Professor Howie Choset. The pictures of the prototypes are shown in figure 2.6. The snake robot is capable to move in 2 dimensional and 3 dimensional. Their investigations are concentrated on planning

movements, developing locomotive algorithms and positioning in what is known as hyper-redundant.

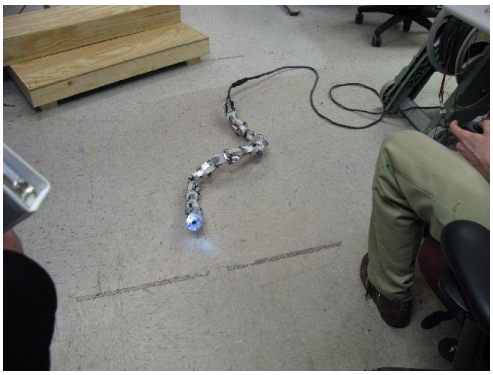

Figure 2.6 CMU snake robot

And they use aluminium modules with a degree of freedom, driven by what is known as Super-servo. These are commercial servos that have been modified, adding their own electronics, sensors and communication bus. Different materials of covers are applied on the snake robot, allowing them to move in all kinds of terrains, including humid area such as pipes. The figure 2.7 shows the different covers and their movements（CMU Biorobotics Lab, 2014）.

Figure 2.7 CMU snake robots with different covers in different terrain

2.3.3 Amphibots at EPFL

The Biorobotics Laboratory in EPFL (Ecole Poly technique Fédérale de Lausanne) has completed some projects to build biologically inspired amphibious snake-like. They developed robots for outdoor robotics tasks taking inspirations from real animals and apply controllers based on the concept of central pattern generators. Their latest generation is AmphibotⅢ, which can swim with speed similar to a human.

Figure 2.8 Amphibots (First, second and third generation)

The first generation, Amphibot-Ⅰ can swim and achieve serpentine locomotion. Its controller presents interesting features such as distributed control, robustness against perturbations, and ability to smoothly adapt the frequency and amplitude of oscillations when control parameters are varied. The type of travelling waves that produce the fastest locomotion gaits using lateral undulation compared with other snake robot at that time (A. Crespi et al., 2004). In second version Amphibot-Ⅱ, the feet were added, then it can swim like salamanders does, combining body and foot movement.

2.3.4 Miller's Snake robot

S5 is one of the most realistic snake robots developed by Miller. It consists of 64 modules with relationship between the length and width of the section nearing the proportions of real snakes. At the beginning, Miller wanted to design a snake robot to enable exploration in dangerous environments and to aid in search and

rescue. Inspired by the python, he finished the simulation on computer. And after several generations of prototypes, finally came to the very mature snake robot S5.

After that, Miller went on the research and modified the design. In 2000 and 2005, the S6 and S7 were accomplished respectively. S6 is made of polycarbonate plastic, brass rod, and plastic gears which make it lighter; and S7 is made of expanded PVC plastic, steel rod, and plastic gears, guaranteeing the light mass as well as the strong structure. In particular it avoids using wheels to achieve locomotion by implementing a more advanced segment design. This allows for rectilinear locomotion. S7 is far more sophisticated electronically than previous snake robots in the series, including bidirectional packet-based radio and a variety of sensors. This information can be found on their website (Snake Robots, 2014).

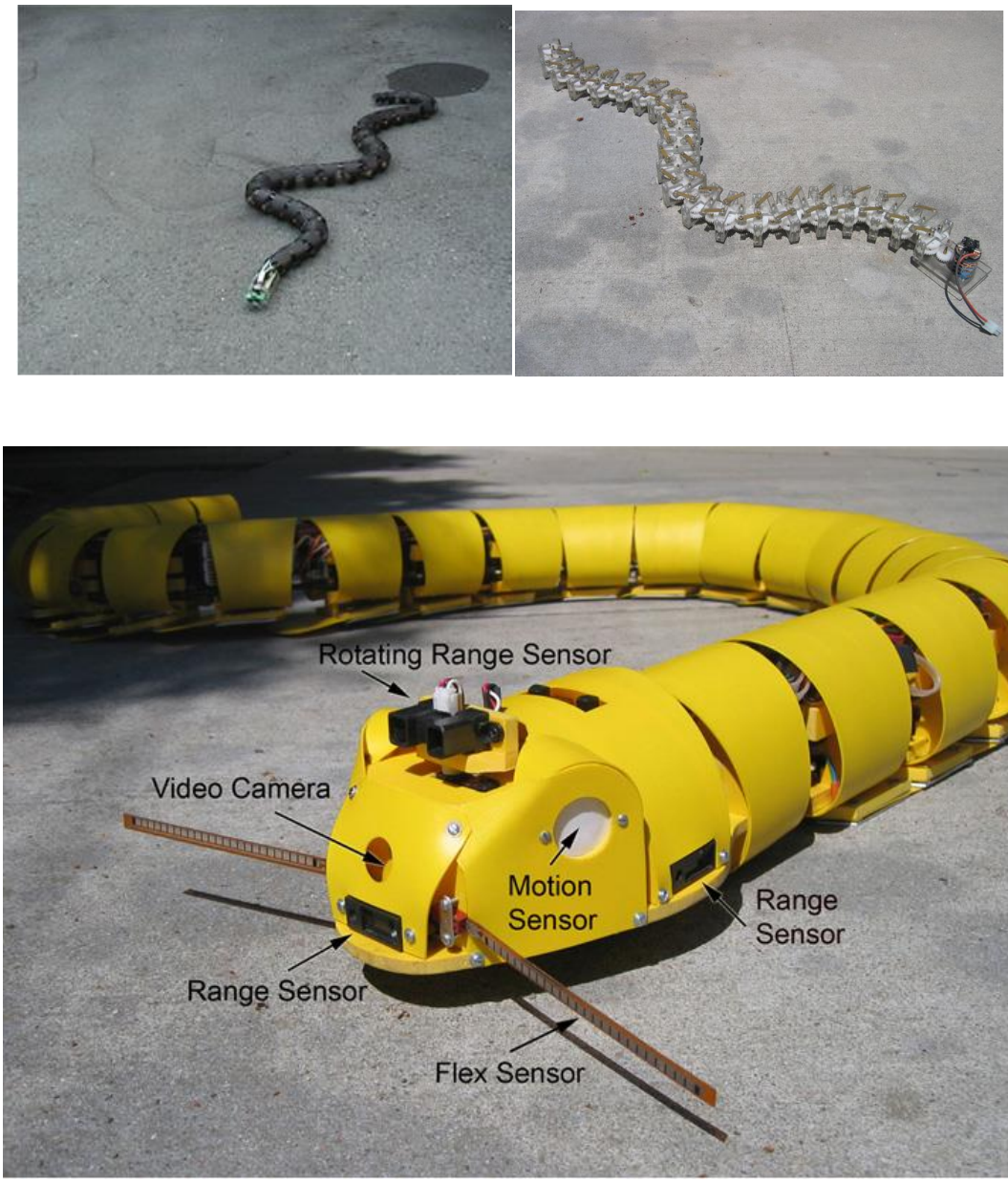

Figure 2.9 Miller's snake robots

2.4 Application of snake robot

Snake robots have some characteristics that make them unique. Advantages contain movement flexibility, self-optimization, and so on. Although it has some merits, but the practical use of snake robot is still on the lab circumstance and being exploring. Normally, from the research by other scientists, the application of snake robot mainly includes search and rescue job, inspection of tubes or bridges and space exploration. The following paragraphs will indicate the researches that have been done in these applications.

2.4.1 Search and rescue

Considering in recent natural disasters and man-made catastrophes, large number of people have died due to inadequate reactive efforts causing by the lack of rescue equipment, and immediate response. Many researchers are searching for the possibility of applying robotic assistant help with rescue operations.

In report about rescue robot by Ismet Erkmen and his fellows (Erkmen et al., 2002), they thought rescue robotics should have the following aspects: detection and identification of living bodies; routing and/or clearing of debris in accessing the victim; physical, emotional, or medical stabilization of the survivor by bringing to him/her automatically administered and tele-metered first aid; fortification of the living body for secure retrieval against any falling debris and possible injuries; transportation of the victim. In order to accomplish these goals, they developed a snake-like prototype with a 12 controllable DOF mechanism. The robot also equipped with an ultrasound sensor and a thermal camera which is

used for detecting and locating. The figure 2.10 shows that, this snake robot can achieve a various modes of locomotion and have been proved in practical.

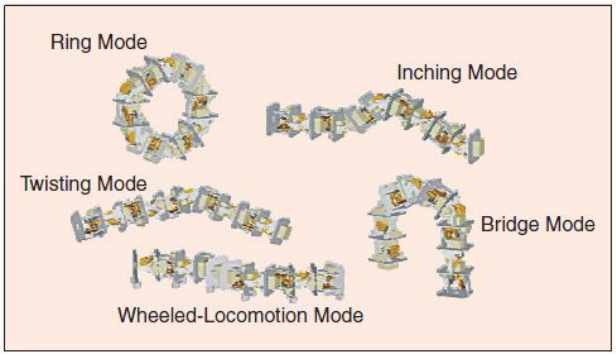

Figure 2.10 Various modes of locomotion

Professor Hirose and Fukushima (Hirose & Fukushima, 2004) come up a paradigm called snake and stings for the rescue operations. This system includes 2 parts: (1) snake-like robot technology for developing information gathering mobile robots, which can thread through the narrow spaces under collapsed buildings; (2) the hyper-tether concept, which can be advantageously applied to assist the snake-like robots, and also to build mobile robot systems that can move and work around disaster sites. They suggested that robots working in groups as a system will be more effective when conducting rescue.

Snake robot “KOHGA”, developed by Tetsushi Kamegawa and his group, and can realize searching under collapsed building by tele-operation; travelling in 3D environment; climbing over obstacle; entering narrow space. It possesses high mobility with various sensors. Figure 2.11 indicates its constitution (Kamegawa et al., 2004).

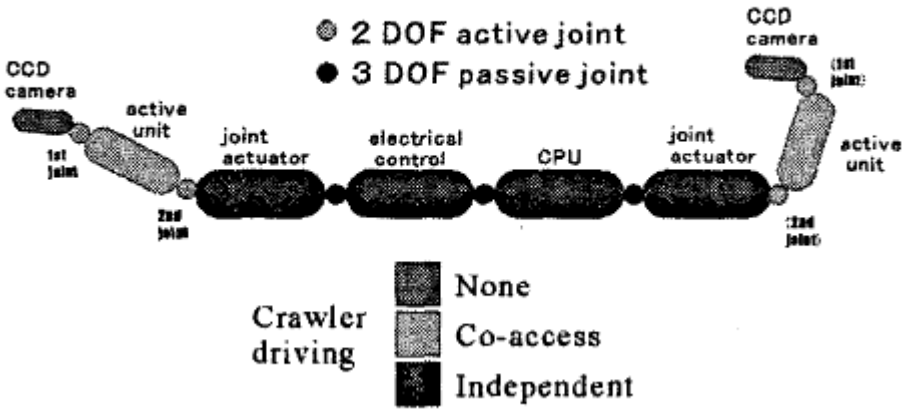

Figure 2.11 Constitution of KOHGA

Also from Japan, Haruo Maruyama and Kazuyuki Ito from Hosei University construct a semi-autonomous snake-like robot which can be controlled in remote place. This machine will supply a lot of help for the volunteer staffs. Because they found that volunteer staffs usually make a great significance during rescue, they almost rescue 70% people after earthquake in Japan. Besides those theoretical analysis, they made an experiment to show their robot performance which is shown in figure 2.12. From the result, this snake-like robot is effective for searching in a wide range of area in a large scale disaster (Maruyam et la., 2010).

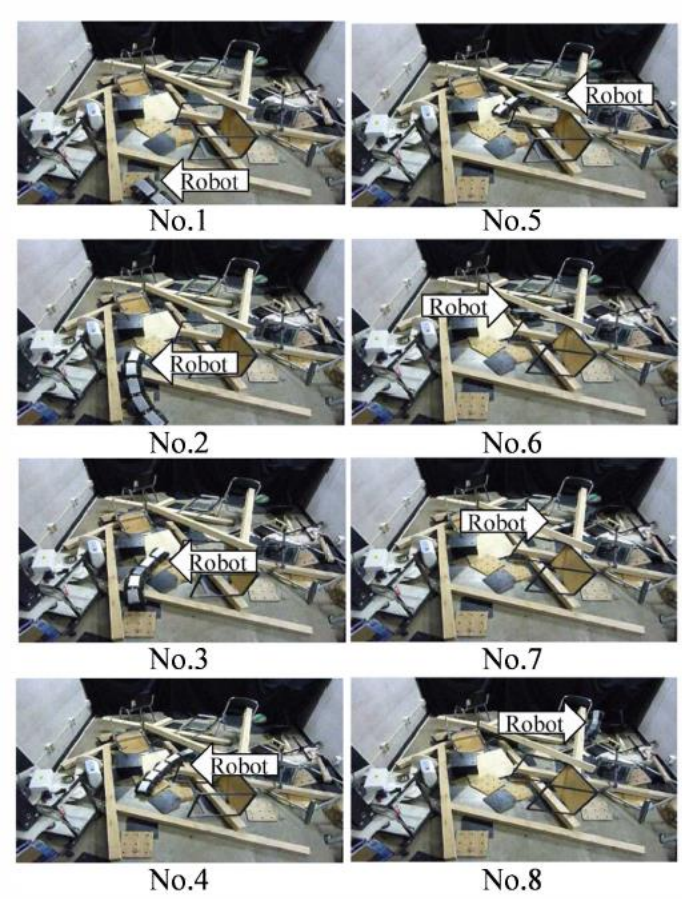

Figure 2.12 Experiment result of rubble

2.4.2 Inspection of tubes or bridges

Another application of snake robot is the inspection of tubes or bridges. Snake robot is suitable to work in these deep and narrow locations where human cannot reach. The Omni Tread serpentine robot design by Malik G. Hansen and Johann Borenstein can accomplish climbing over high steps, travelling inside or outside of horizontal or even vertically pipes (Granosik et al., 2005).

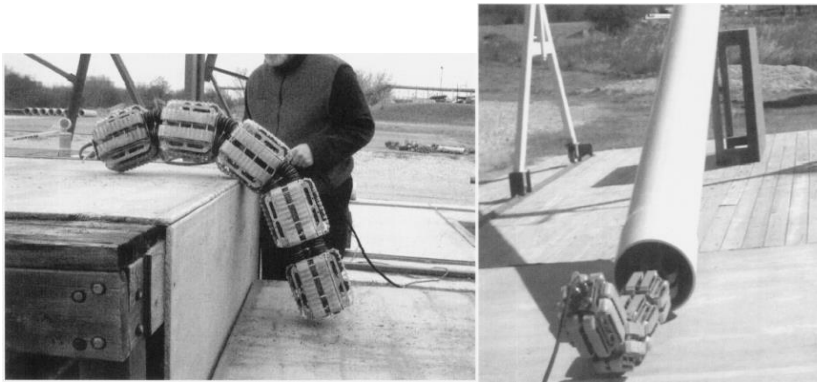

Figure 2.13 Omni Thread serpentine robot climbs 66cm step and crosses a PVC pipe

GMD-Snake is built by K.L.Paap and T.Christaller to inspect broken buildings, the second generation--Snake 2 is made of five identical sections which are connected via universal joints just as figure 2.14 shows. What make difference is that a ring of wheels are implemented on each joint, and these wheels can be activated by additional DC motor per section. This design enables a great flexibility to the snake robot when moving. It can move not only in serpentine motion but also be driven by active wheels (Paap K.L et al., 2000).

Figure 2.14 GMD-Snake 2 with 5 sections

PIKo is a mechanism for navigating complex pipe structures, both horizontally and vertically. Horizontal motion is achieved by the propulsion wheels on each

module, and vertical motion is achieved by spanning the pipe alternating with the modules. The figure 2.15 shows its configuration.

Figure 2.15 The pipe inspection robot PIKo

Researchers also implemented experiments on the robot vertical climbing and got a successful result. They developed a wireless controller for the robot so that it can be controlled in remote place (Fjerdingen et al., 2009).

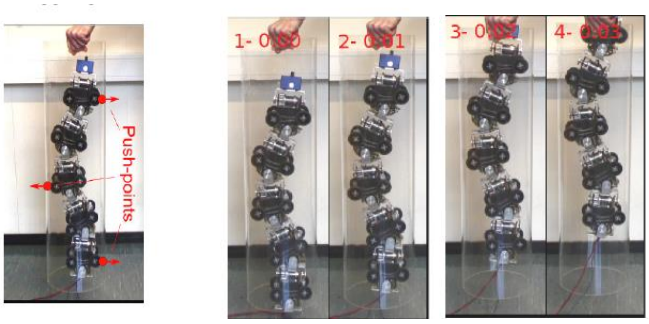

Figure 2.16 The vertical motion experiments of PIKo

2.5 Analysis

In former paragraphs, researches of snake robot around the word have been introduced. With some significant advantages, snake robots have potential to be a perfect assistant in rescue operations and inspection tasks. Research challenges are related to two aspects: development of physical snake robots, modelling and controlling of snake robots (P.Liljebäck et al., 2012).Though excellent prototypes

have been designed and made by the scientists, the applications of snake robot are mainly in laboratorial scale.

In the previous snake robot researches, the serpentine locomotion is the majority kind of motion applied by snake robot, no matter how the control method is, due to its moving efficiency and easy approaching. Another issue is that no actual field experience has been done by snake robot in search and rescue operations. All the proposals are just in concept stage or in the simulation laboratorial scale and none of them applied the sensors to guide the movement and accomplish the information gathering. This motivated my study to install a camera on a snake robot to perform the search operation.

The work will be started with the theory study and equation deducing. After that, snake robot simulation is a significant tool to prove the built mathematical model. Accomplishing the simulation work helps the program writing task. The hardware part of the snake robot has been finished, so a model will be built in simulation platform which is V-REP. Finally, applying workable controlling code in the implementation to check the result.

Chapter 3. Kinematics and dynamics model of snake robot

3.1 Kinematics

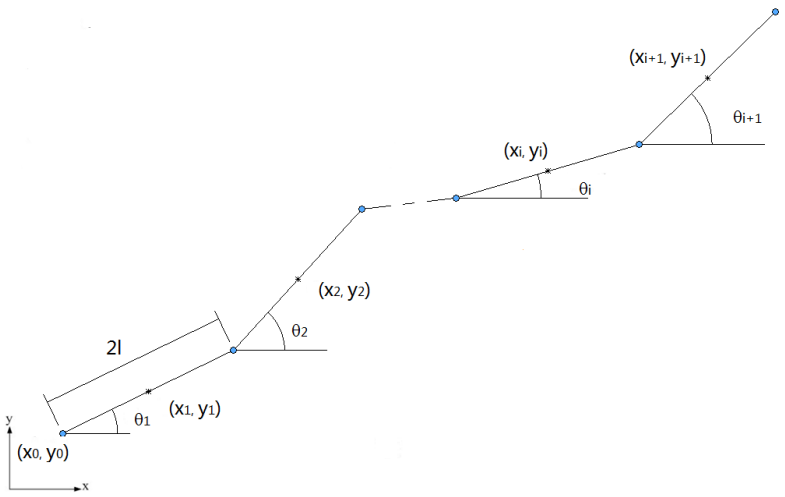

Figure 3.1 Snake robot model

A simplified model of snake robot is built in plane coordinates with the head at (x_0, y_0). The length and weight of each segment are the same, which are 2l and m respectively. Assuming that the centre of gravity (x_i, y_i) of segment is in the centre of every joint. Hence, the model is showed in figure 3.1

The parameters are defined as follow:

$2l$: the length of each segment;

l : Length between the joint and centre of gravity;

θ_i : The absolute angle between ith segment and x coordinate;

$\emptyset_i$: Relative angle at joint i;

(x_0, y_0): The position of the snake head;

(x_i, y_i) : The position of the ith segment centre of gravity.

According to the figure 3.1, the equation of ith segment gravity position can be written as equation (3.1).

$$x_i = x_0 + 2l \sum_{j=1}^{i-1} \cos\theta_j + l\cos\theta_i$$

$$y_i = y_0 + 2l \sum_{j=1}^{i-1} \sin\theta_j + l\sin\theta_i$$

where i= 1, 2, 3, ⋯, n (3.1)

Differentiating this equation to yield velocity of ith segment:

$$\dot{x_ı} = \dot{x_0} - 2l \sum_{j=1}^{i-1} \dot{\theta_j} \sin\theta_j - l\dot{\theta_ı}\sin\theta_i$$

$$\dot{y_ı} = \dot{y_0} + 2l \sum_{j=1}^{i-1} \dot{\theta_j} \cos\theta_j + l\dot{\theta_ı}\cos\theta_i$$

where i= 1, 2, 3, ⋯, n (3.2)

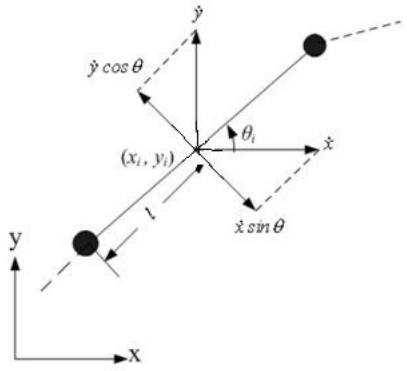

Figure 3.2 The no slip limitation of segment i

In order to make sure that no slip happens during the snake motion, a limitation is introduced as figure 3.2.

$$\dot{x}_i \sin\theta_i - \dot{y}_i \cos\theta_i = 0$$

where i= 1, 2, 3, ⋯, n (3.3)

Substitute (3.2) into (3.3), then

$$\dot{y_0} \cos\theta_i - \dot{x_0} \sin\theta_i + l\dot{\theta}_i + 2l \sum_{j=1}^{i-1} \dot{\theta}_j \cos(\theta_i - \theta_j) = 0$$

where i= 1, 2, 3, ⋯, n (3.4)

Rewrite the equation (3.4) in matrix form:

$$[F_A - F_B] \begin{bmatrix} \dot{\theta}_i \\ \dot{r} \end{bmatrix} = 0$$

where

$$F_A = \begin{bmatrix} 1 & 0 & 0 & 0 & 0 & 0 \\ 2l\cos(\theta_2-\theta_1) & 1 & 0 & 0 & 0 & 0 \\ 2l\cos(\theta_3-\theta_1) & 2l\cos(\theta_3-\theta_2) & 1 & 0 & 0 & 0 \\ \vdots & \vdots & & \ddots & 0 & 0 \\ 2l\cos(\theta_{n-1}-\theta_1) & 2l\cos(\theta_{n-1}-\theta_2) & \cdots & 2l\cos(\theta_{n-1}-\theta_{n-2}) & 1 & 0 \\ 2l\cos(\theta_n-\theta_1) & 2l\cos(\theta_n-\theta_2) & \ldots & 2l\cos(\theta_n-\theta_{n-2}) & 2l\cos(\theta_n-\theta_{n-1}) & 1 \end{bmatrix} \in R^{n\times n}$$

$$F_B = \begin{bmatrix} \sin\theta_1 & -\cos\theta_1 \\ \sin\theta_2 & -\cos\theta_2 \\ \vdots & \vdots \\ \sin\theta_n & -\cos\theta_n \end{bmatrix} \in R^{n\times 2},\ \dot{\theta}_1 = \begin{bmatrix} \dot{\theta}_1 \\ \dot{\theta}_2 \\ \vdots \\ \dot{\theta}_n \end{bmatrix},\ \dot{r} = \begin{bmatrix} \dot{x}_0 \\ \dot{y}_0 \end{bmatrix} \tag{3.5}$$

Rearranging the terms yields:

$$[I_n - F_\theta]\begin{bmatrix} \dot{\theta}_1 \\ \dot{r} \end{bmatrix} = 0$$

where $F_\theta = {F_A}^{-1}F_B \in R^{n\times 2}$, $[I_n - F_\theta] \in R^{n\times(n+2)}$ (3.6)

3.2 Dynamics

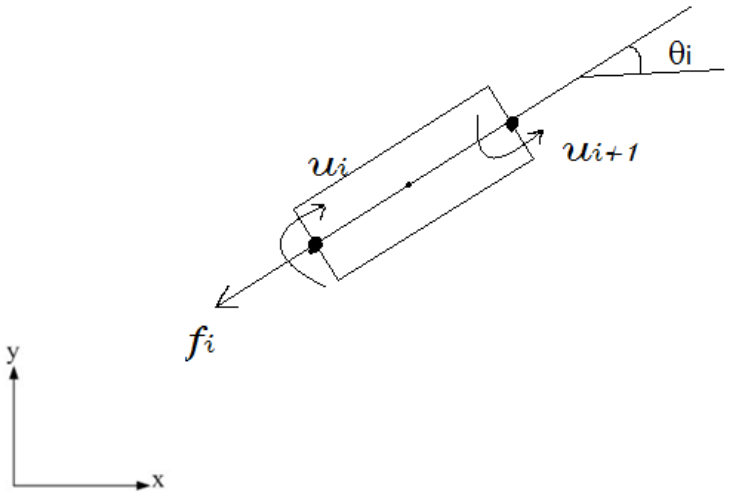

Figure 3.2 Dynamic model of segment i

A snake with n segments has n-1 joints, consider the ith segment of the snake robot with torque u_i and friction f_i at joint i as shown in figure 3.2.

Let $u = \begin{bmatrix} u_1 \\ u_2 \\ \vdots \\ u_{n-1} \end{bmatrix} \in R^{n-1}$ be the control torque, $f = \begin{bmatrix} f_1 \\ f_2 \\ \vdots \\ f_n \end{bmatrix} \in R^n$ be the matrix of friction.

The kinetic energy T:

$$T = \frac{1}{2}\sum_{i=1}^{n}\left[m\left(\dot{x_i}^2 + \dot{y_i}^2\right) + J\dot{\theta_i}^2\right]$$

$$= \frac{1}{2}\dot{q}^T M(\theta)\dot{q} \tag{3.7}$$

where $q = \begin{bmatrix} \theta \\ r \end{bmatrix} \in R^{n+2}$

$M(\theta)$ is a (n+2)×(n+2) positive definite symmetric geometry inertia matrix of the snake robot.

Potential energy U is 0, since the robot is assumed to locomote on the x-y plane.

Dissipation energy of the snake robot:

$$D = \frac{1}{2}\sum_{i=1}^{n-1} d_\theta \cdot \dot{\theta_i}^2 \tag{3.8}$$

where d_θ is the damping constant of the revolute joint.

As a result, the dissipation energy can be rewritten as

$$D = \frac{1}{2}\dot{q}^T N\dot{q} \tag{3.9}$$

where N is a (n+2)×(n+2) matrix

$$N = \begin{bmatrix} d_\theta & -d_\theta & 0 & 0 & \cdots & 0 & 0 & 0 & 0 & 0 \\ -d_\theta & 2d_\theta & -d_\theta & 0 & \cdots & 0 & 0 & 0 & 0 & 0 \\ 0 & -d_\theta & 2d_\theta & -d_\theta & \cdots & 0 & 0 & 0 & 0 & 0 \\ \vdots & \vdots & \vdots & \vdots & \ddots & \vdots & \vdots & \vdots & \vdots & \vdots \\ 0 & 0 & 0 & 0 & \cdots & -d_\theta & 2d_\theta & -d_\theta & 0 & 0 \\ 0 & 0 & 0 & 0 & \cdots & 0 & -d_\theta & d_\theta & 0 & 0 \\ 0 & 0 & 0 & 0 & \cdots & 0 & 0 & 0 & 0 & 0 \\ 0 & 0 & 0 & 0 & \cdots & 0 & 0 & 0 & 0 & 0 \end{bmatrix} \in R^{(n+2)\times(n+2)}$$

The general Eula-Lagrange equation is expressed as

$$\frac{d}{dx}\frac{\partial L}{\partial \dot{q}_\imath} - \frac{\partial L}{\partial q_i} + \frac{\partial D}{\partial q_i} = Q_i + \tau_i$$

where i = 1, 2, ⋯ , n (3.10)

$L = T - U$ is the Lagrangian of the snake robot.

Q_i is the generalised force including all the external non-conservative force by the environment, τ_i is the actuator torque in the generalised coordinate.

Since $\emptyset_i = \theta_{i+1} - \theta_i, \ \forall i = 1, 2, \cdots n$

in matrix form: $\emptyset = E^T\theta$ (3.11)

and $E^T = \begin{bmatrix} -1 & 1 & 0 & \cdots & 0 \\ 0 & -1 & 1 & \cdots & 0 \\ \vdots & \vdots & \vdots & \ddots & \vdots \\ 0 & 0 & \cdots & 1 & 0 \\ 0 & 0 & \cdots & -1 & 1 \end{bmatrix}$

By the principle of virtual work

$u_\theta{}^T \partial\theta = u_\emptyset{}^T \partial\emptyset$ (3.12)

where u_θ and $u_\emptyset$ are the actuator torques in generalised coordinate space and joint space respectively.

Let τ be the torque in generalised coordinate, then:

$$\tau = \begin{bmatrix} \tau_1 \\ \vdots \\ \tau_n \\ \tau_{n+1} \\ \tau_{n+2} \end{bmatrix} = \begin{bmatrix} Eu \\ 0 \\ 0 \end{bmatrix} \tag{3.13}$$

where E is the transform matrix between the absolute actuator angle and the joint angle

Substituting equations (3.10) and (3.11) into (3.13), yields the equation of motion

$$M(\theta)\ddot{q} + C\left(\dot{\theta}, \theta\right)\dot{q} + N\dot{q} = Q + \tau \tag{3.14}$$

where

$$M(\theta) = \begin{bmatrix} (4n-3)ml^2 + J & 2(n+2)ml^2\cos(\theta_2 - \theta_1) & \cdots & & & \\ 2(n+2)ml^2\cos(\theta_2 - \theta_1) & [(4(n-1)-3)]ml^2 + J & \cdots & & \text{Symmertric} & \\ \vdots & \vdots & \ddots & & & \\ 6ml^2\cos(\theta_{n-1} - \theta_1) & 6ml^2\cos(\theta_{n-1} - \theta_2) & \cdots & 5ml^2 + J & & \\ 2ml^2\cos(\theta_n - \theta_1) & 2ml^2\cos(\theta_n - \theta_2) & \cdots & 2ml^2\cos(\theta_n - \theta_{n-1}) & ml^2 + J & \\ -(2n-1)ml\sin\theta_1 & -[2(n-1)-1]ml\sin\theta_2 & \cdots & -3ml\sin\theta_{n-1} & -ml\sin\theta_n & nm \quad 0 \\ -(2n-1)ml\cos\theta_1 & -[2(n-1)-1]\cos\theta_2 & \cdots & -3ml\cos\theta_{n-1} & ml\cos\theta_n & 0 \quad nm \end{bmatrix}$$

$$\in R^{(n+2)\times(n+2)}$$

$C\left(\dot{\theta}, \theta\right)$=

$$\begin{bmatrix} 0 & 2(n+2)ml^2\sin(\theta_2 - \theta_1)\dot{\theta_2} & 2[(n-2)+2]ml^2\sin(\theta_3 - \theta_1)\dot{\theta_3} & \cdots & \cdots & 6ml^2\sin(\theta_{n-1} - \theta_1)\dot{\theta_{n-1}} & 2ml^2\sin(\theta_n - \theta_1)\dot{\theta_n} \\ & 0 & 2[(n-2)+2]ml^2\sin(\theta_3 - \theta_2)\dot{\theta_3} & \cdots & \cdots & 6ml^2\sin(\theta_{n-1} - \theta_2)\dot{\theta_{n-1}} & 2ml^2\sin(\theta_n - \theta_2)\dot{\theta_n} \\ & & 0 & \ddots & \cdots & \vdots & \vdots \\ & & & & 0 & 6ml^2\sin(\theta_{n-1} - \theta_{n-2})\dot{\theta_{n-1}} & 2ml^2\sin(\theta_n - \theta_{n-2})\dot{\theta_n} \\ & & \text{Symmertric} & & & 0 & 2ml^2\sin(\theta_n - \theta_{n-1})\dot{\theta_n} \\ & & & & & & 0 \end{bmatrix}$$

$C(\dot{\theta}, \theta)$ is the Corilis matrix of the snake robot while $C(\dot{\theta}, \theta)\dot{q}$ represents the Corilis and centrifugal force.

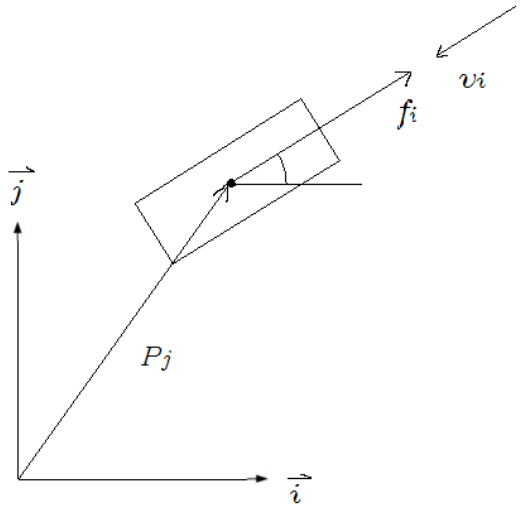

Figure 3.3 The generalised force on the segment i

Figure 3.3 shows the friction force between the ith segment and the x-y plane.

The generalised force Q_i is expressed as:

$$Q_i = \sum_j^k f_j \frac{\partial P_j}{\partial q_i}$$

where i= 1, 2, ⋯, n, n+1, n+2 (3.15)

$P_j = x_j\vec{\mathbf{i}} + y_j \underset{j}{\rightarrow}$ (j=1, 2, ⋯, n) is the point of applied friction f_j, where $f_j = f_j\cos\theta_j \underset{i}{\rightarrow} + f_j\sin\theta_j \underset{j}{\rightarrow}$.

Hence the generalised force Q_i is expressed as:

$$Q_{n-k} = \sum_{j=1}^k 2lf_{n-j+1}\sin(\theta_{n-j+1} - \theta_{n-k}) \quad k=1, 2, \cdots, n-1 \qquad (3.16)$$

$$\vdots$$

$$Q_n = 0 \tag{3.17}$$

$$Q_{n+1} = \sum f_i \cos\theta_i \qquad i=1, 2, \cdots, n \tag{3.18}$$

$$Q_{n+2} = \sum f_i \sin\theta_i \qquad i=1, 2, \cdots, n \tag{3.19}$$

Combining equations (3.16), (3.17), (3.18) and (3.19)gives the matrix Q

$$Q = G(\theta)f \tag{3.20}$$

where

$$G(\theta) = \begin{bmatrix} 0 & 2l\sin(\theta_2 - \theta_1) & 2l\sin(\theta_3 - \theta_1) & \cdots & 2l\sin(\theta_n - \theta_1) \\ 0 & 0 & 2l\sin(\theta_3 - \theta_2) & \cdots & 2l\sin(\theta_n - \theta_2) \\ 0 & 0 & 0 & \cdots & \vdots \\ \vdots & \vdots & \vdots & \ddots & 2l\sin(\theta_n - \theta_{n-1}) \\ 0 & 0 & 0 & \cdots & 0 \\ \cos\theta_i & \cos\theta_i & \cos\theta_i & \cdots & \cos\theta_i \\ \sin\theta_i & \sin\theta_i & \sin\theta_i & \cdots & \sin\theta_i \end{bmatrix}$$

Merging equation (3.14) with the kinematic equation (3.6) by Lagrange multiple

$$\lambda = \begin{bmatrix} \lambda_1 \\ \vdots \\ \lambda_{n+2} \end{bmatrix} \in R^{n+2}$$

gives:

$$M(\theta)\ddot{q} + C(\dot{\theta}, \theta)\dot{q} + N\dot{q} - \begin{bmatrix} Eu \\ 0 \\ 0 \end{bmatrix} - \begin{bmatrix} I_n \\ -F^T_{(\theta)} \end{bmatrix} \lambda = Q \tag{3.21}$$

From equation (3.6), $\dot{\theta} = F\dot{r}$

$$\ddot{\theta} = \dot{F}\dot{r} + F\ddot{r} \tag{3.22}$$

Hence equations (3.21) becomes

$$[F^T I_2]M(\theta)\begin{bmatrix}\dot{F}\dot{r} + F\ddot{r}\\ \ddot{r}\end{bmatrix} + [F^T I_2]C(\dot{\theta},\theta)\begin{bmatrix}\dot{F}\dot{r}\\ \dot{r}\end{bmatrix} + [F^T I_2]N\begin{bmatrix}\dot{F}\dot{r}\\ \dot{r}\end{bmatrix} - [F^T I_2]\begin{bmatrix}Eu\\ 0\\ 0\end{bmatrix} -$$

$$[F^T I_2]\begin{bmatrix}I_n\\ -F^T{}_{(\theta)}\end{bmatrix}\lambda = [F^T I_2]G(\theta)f \tag{3.23}$$

Rearranging the items gives

$$M'(\theta)\ddot{r} + C'(\dot{\theta},\theta)\dot{r} + N'\dot{r} - F^T Eu = [F^T I_2]G(\theta)f \tag{3.24}$$

Where

$$M'(\theta) = [F^T I_2]M(\theta)\begin{bmatrix}F\\ I_2\end{bmatrix} \in R^{2\times 2}$$

$$C'(\dot{\theta},\theta) = [F^T I_2]C(\dot{\theta},\theta)\begin{bmatrix}F\\ I_2\end{bmatrix} + [F^T I_2]M(\theta)\begin{bmatrix}\begin{bmatrix}0 & F\\ 0 & 0\end{bmatrix}\end{bmatrix} \in R^{2\times 2}$$

$$N' = [F^T I_2]N\begin{bmatrix}F\\ I_2\end{bmatrix} \in R^{2\times 2}$$

3.3 Serpenoid Curve

3.3.1 Continuous serpenoid curve

Serpenoid curve was introduced by Hirose (Hirose, 1993) for describing the body shape of a snake during the most common locomotion of lateral undulation. The propulsion of the snake robot is mainly due to the curvature of the body shape.

The main features of a serpenoid curve is its sinusoidal variation of curvature.

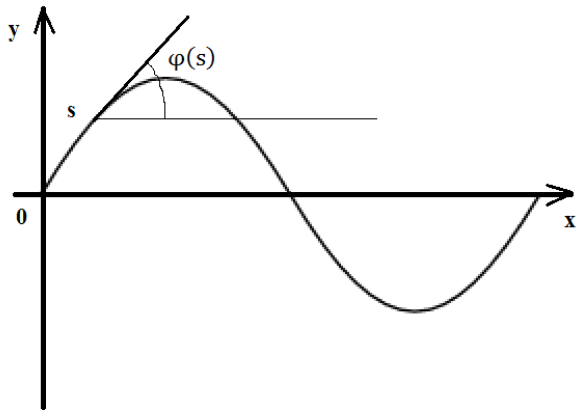

Figure 3.4 Tangential angle at point s

The curvature of a serpenoid curve is given as

$$K(s) = -a\frac{2K_n\pi}{L}\sin(\frac{2K_n\pi}{L}s) \tag{3.25}$$

where

s is the curve length

a is the initial winding angle (which is the tangential angle φ at s=0)

K_n is the number of sine-shapes in the curve

L is the total curve length

The tangential angle at s shown in figure 3.4 is obtained by integrating equation (3.26)

$$\varphi(s) = a\cos(\frac{2K_n\pi}{L}s) \tag{3.26}$$

The serpenoid curve are give as:

$$x(s) = \int_0^s \cos(\varphi(\sigma))\, d\sigma$$

$$y(s) = \int_0^s \sin(\varphi(\sigma))\, d\sigma \tag{3.27}$$

where $(x(s), y(s))$ is the point on the serpenoid curve

The serpenoid curve oscillates about the line of symmetry. In order to control the line of symmetry of the curve, a constant c is introduced into the curve. Such that

$$K(s) = -a\frac{2K_n\pi}{L}\sin(\frac{2K_n\pi}{L}s) + c \tag{3.28}$$

While the tangential angle become

$$\varphi(s) = a\cos(\frac{2K_n\pi}{L}s) + cs$$

Hence, the serpenoid curve is expressed as

$$x(s) = \int_0^s \cos(a\cos(\frac{2K_n\pi}{L}s) + cs)\, ds$$

$$y(s) = \int_0^s \sin(a\cos(\frac{2K_n\pi}{L}s) + cs)\, ds \tag{3.29}$$

Figure 3.5, 3.6 and 3.7 show the parameters a, K_n and c affect the serpenoid curve shape.

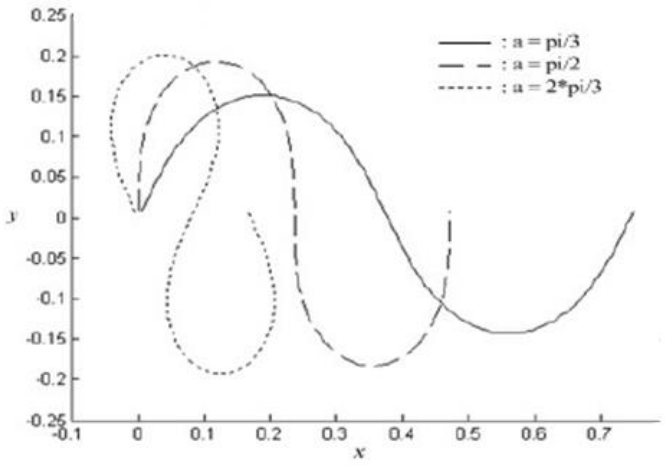

Figure 3.5 Different a with K_n=1, c=0

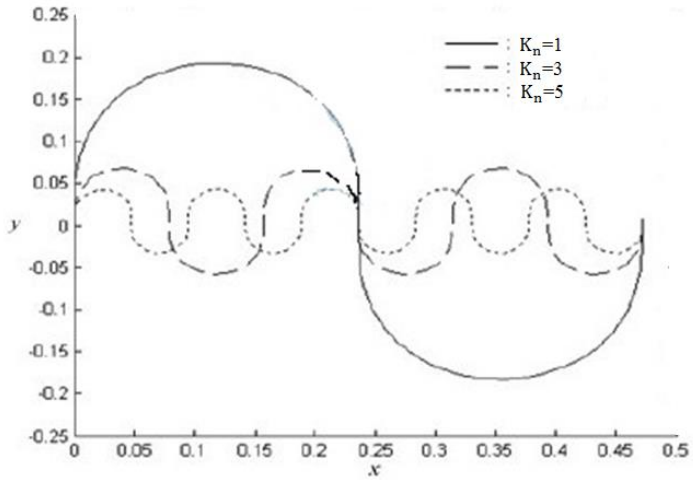

Figure 3.6 Different K_n with a=pi/2, c=0

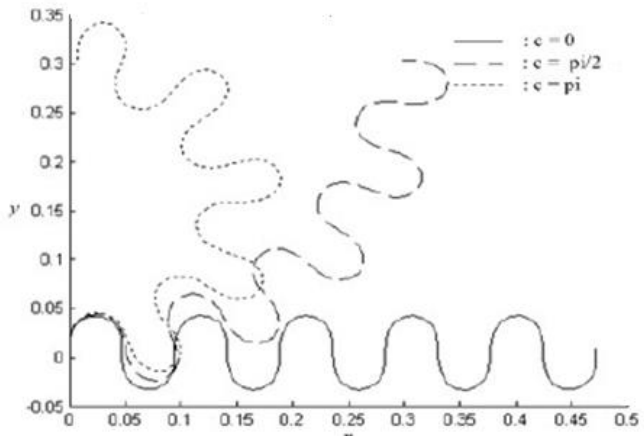

Figure 3.7 Different c with a=pi/2, K_n=5

3.3.2 Discrete serpenoid curve

Discretizing the serpenoid curve into n segments and assuming the total length of curve is 1, such that the length of a segment is $\frac{1}{n}$. As a result, $s_i = \frac{i}{n}$, ∀i=0,1, ⋯, n.

The curve is represented by n+1 segment joint points with the first point at (x_0, y_0) and n points from i=1 to i=n.

$$x_i = \sum_{j=1}^{i} \frac{1}{n} \cos\left(a \cos\left(\frac{2K_n \pi}{L} \frac{j}{n}\right) + c \frac{j}{n}\right)$$

$$y_i = \sum_{j=1}^{i} \frac{1}{n} \sin\left(a \cos\left(\frac{2K_n \pi}{L} \frac{j}{n}\right) + c \frac{j}{n}\right)$$

where i=1, 2, ⋯, n. (3.30)

The joint angle θ_i is given as

$$\tan \theta_i = \frac{y_i - y_{i-1}}{x_i - x_{i-1}}$$

which yields

$$\theta_i = a\cos\left(\frac{i}{n}\cdot\frac{2K_n\pi}{L}\right) + \frac{i}{n}c \tag{3.31}$$

The relative angle between joint i and joint (i+1) is

$$\emptyset_i = \theta_i - \theta_{i-1}$$

$$= \alpha\sin\left(i\beta + \frac{\beta}{2}\right) + \gamma \tag{3.32}$$

Where $\alpha = 2a\left|\sin\frac{\beta}{2}\right|$

$$\beta = \frac{2K_n\pi}{L}\frac{1}{n}$$

$$\gamma = -\frac{c}{n}$$

Thus, the relative angle $\emptyset_i$ changes in a sinusoidal manner along the "discrete arc length" i/n with the amplitude α and the bias γ. Any two adjacent relative angles have the phase difference β. So the parameters can be explained:

α : determine the amplitude of sine equation;

β : determine the phase difference between the joint in sequence, and they are all the same.

γ : determine the deviation angle with x coordinate.

Thus, the relative angle can be approximately written in a time t dominion with the angular velocity of the sinusoidal manner ω.

$\emptyset_i(t) = \alpha\sin(\omega t + (i-1)\beta) + \gamma$, where i= 1, 2, 3,..., n-1. (3.33)

The absolute joint angle θ can be calculated from equation (3.11) with the relative joint angle given by equation (3.33).

Therefore, the snake robot motion can be derived while providing the shape change through the joint variables $\theta(t)$, $\dot{\theta}(t)$ and $\ddot{\theta}(t)$.

Equation (3.6) yields $\dot{r}$ from $\dot{\theta}$ and $\ddot{r}$ is obtained by differential. Substituting these variables into equation (3.24) to calculate the required torque provided by the actuator.

Chapter 4. Modification of serpenoid motion and simulation

4.1 Issues about the serpenoid curve

The snake robot is designed for search and rescue operations, and a wireless camera is installed on the head of snake robot as a visual system. The function of visual system is not only to gather the information; it also feeds the information back to the remote control operator to control the snake robot moving direction.

Figure 4.1 indicates the moving direction and the camera sight direction. Both directions make an angle γ and θ_1 with the x-axis respectively. Since the snake robot head is travelling along the serpenoid curve as its body is moving along the moving direction γ, its line of sight has the same orientation as the tangent to the curve. Hence, the camera sight direction aligning with the line of sight is oscillating along the serpenoid curve too. It results the swinging video images received from the camera, which is not desirable for gathering information and controlling moving direction.

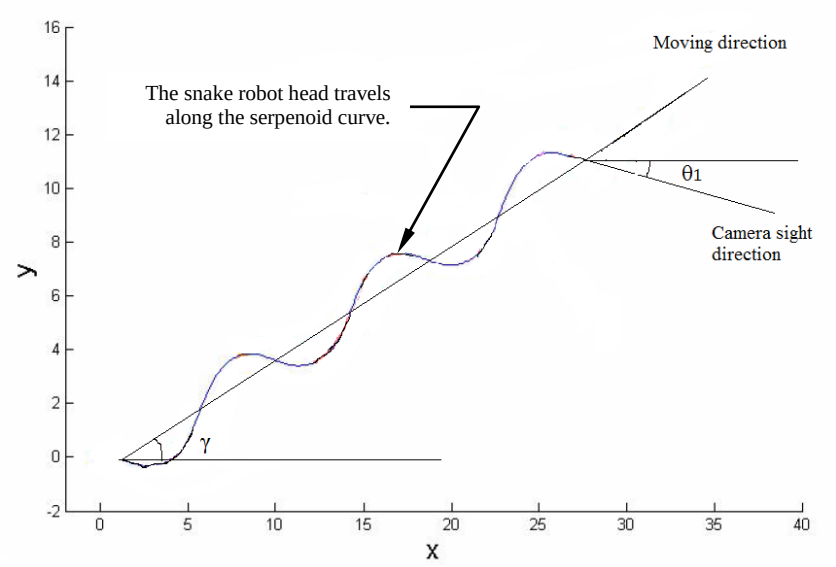

Figure 4.1 The relationship between the moving direction and sight of camera

4.2 Simulation of normal serpentine locomotion

The model of snake robot is built in this part and serpentine locomotion is simulated in a robotic simulation software V-REP to show the camera swing.

4.2.1 Modelling

The snake robot is composed of 9 segments and 8 joints. The first segment is the head and joint 1 links the head with the body. As the V-REP is not user-friendly for 3D modelling, the snake robot is built in Solidworks and then transferred to V-REP.

Figure 4.2 The model built in Solidworks

Figure 4.2 shows the snake robot model built in Solidworks, 9 segments is linked by 8 joints and each joint contains 2 motors which enable the joint to rotate in vertical and horizontal direction respectively.

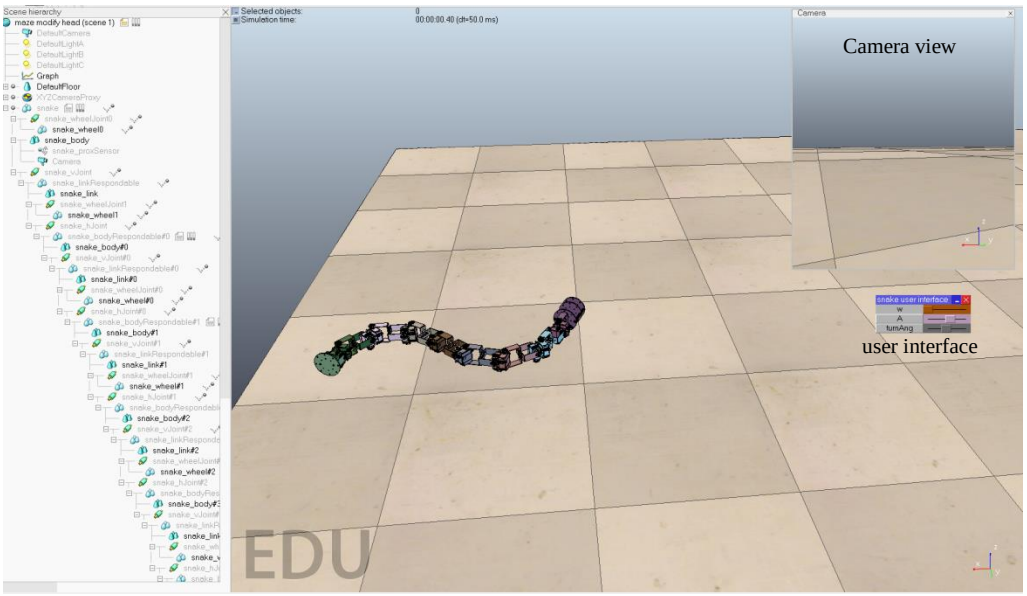

Figure 4.3 The model rebuilt in V-REP

The Solidworks model is imported into V-REP and then is rebuilt to make it as a dynamic snake robot model, settings are shown in appendix A. Figure 4.3 presents the result rebuilt model in V-REP. A camera is attached on the snake robot head.

The video images collected by the camera is shown in a floating view located on the top right corner of the figure. A user interface with three sliders for controlling the snake robot is also shown in the right hand side of the figure and is enlarged in Figure 4.4.

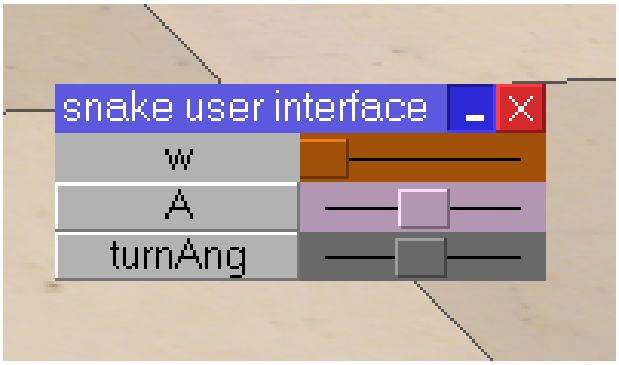

Figure 4.4 Controlling interface

In the interface, "w" (which is ω in the equation (3.33)) controls the snake moving speed. "A" (which is the "α" in equation (3.33)) controls the amplitude of the serpenoid motion while "turnAng" (which is the“γ”in equation (3.33)) determines the snake robot moving direction.

4.2.2 Serpentine locomotion simulation

The snake robot in the simulation software V-REP employs individual virtual controller (which is expressed in terms of the script language) for each joint. The control strategy is that each segment controls its own joints’ movement, and together with a specified movement of all the joints, the snake will move along the serpenoid curve. So, eight scripts are built to control the relative angle$\emptyset_i(t)$ (i = 1, 2, …, 8) of each joint individually.

The serpenoid curve equation which deduced in the previous chapter is $\emptyset_i(t) = \alpha \sin(\omega t + (i-1)\beta) + \gamma$, where i= 1, 2, 3,..., n-1, $\alpha = 2a\left|\sin\frac{\beta}{2}\right|$, $\beta = \frac{2K_n\pi}{L}\frac{1}{n}$, $\gamma = -\frac{c}{n}$.

The number of undulation of snake robot is set as 1 and winding angle is set as pi/3, then a=$\frac{\pi}{3}$, K_n=1. Substituting a=$\frac{\pi}{3}$, K_n=1 into the equation yields

$$\emptyset_i(t) = 41.04 \sin(-\omega t + (i-1)\frac{2\pi}{9}) + \gamma. \quad (4.1)$$

A negative sign before the time t is added to get the required moving direction under control.

Figure 4.5 presents the simulation result for the snake robot locomotion in one cycling and the camera sight direction from the head of snake robot is also shown in the figure as a red line (which is the line of sight).

The snake robot is simulated to move toward the right hand side. The head direction and the camera sight oscillates from pointing to the top right corner at the beginning (t = 0) to low right corner at t = π, and then swings back to top right corner at t = 2π.

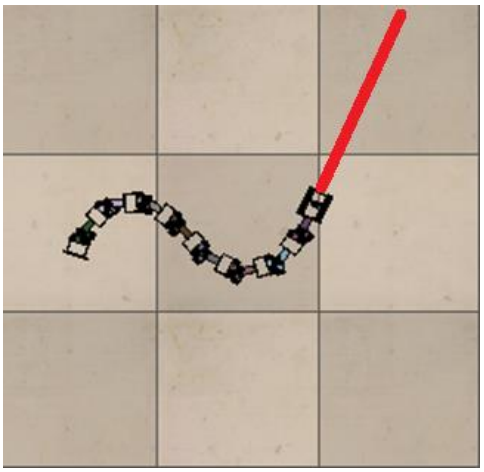

t = 0

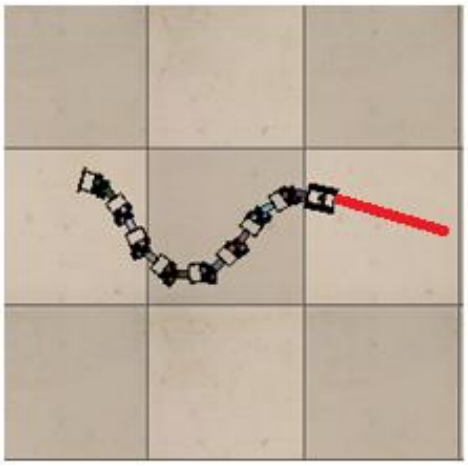

t = $\frac{\pi}{2}$

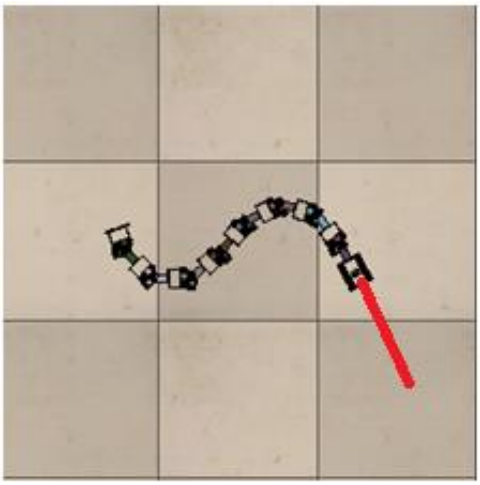

t = π

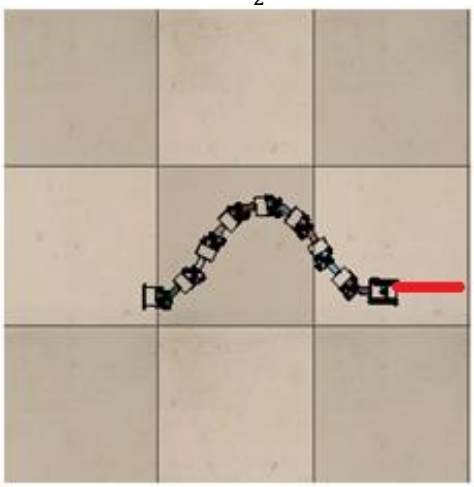

t = $\frac{3\pi}{2}$

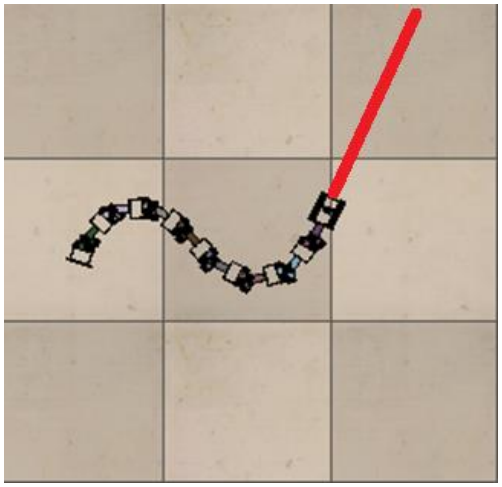

t = 2π

Figure 4.5 The snake robot shape in one cycling

In order to show the swinging clearly in the camera sight, six cubes numbered from 1 to 6 aligning in the same y position are inserted in front of the snake during locomotion as shown in figure 4.6. The camera sight at the beginning of locomotion (t = 0) only covers the cube 1 in the figure 4.6 (a) which is shown in the camera view on the top right comer. With the snake moving forward, the camera covers cube 3, 4 and 5 in figure 4.6 (b) at t = $\frac{\pi}{2}$ as shown in the camera view and then only capture cube 6 in figure 4.6 (c) at t = π. The cube 3, 4 and 5 are shown in the camera view again as the snake robot head oscillates back at t = $\frac{3\pi}{2}$. Finally, the cube 1 and 2 in figure 4.6 (e) are captured by the camera t = 2π.

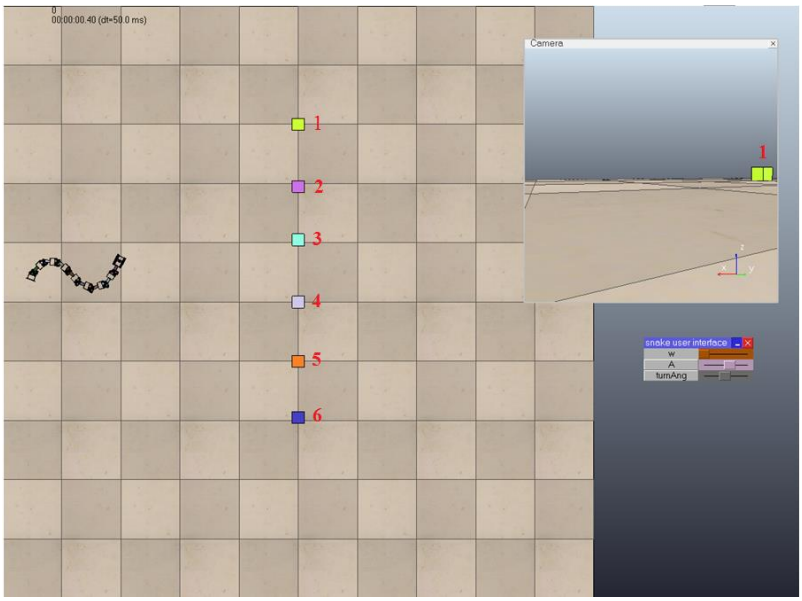

(a) t = 0

Figure 4.6 The camera sight of snake robot when moving forward
(continue on next page)

(b) t = $\frac{\pi}{2}$

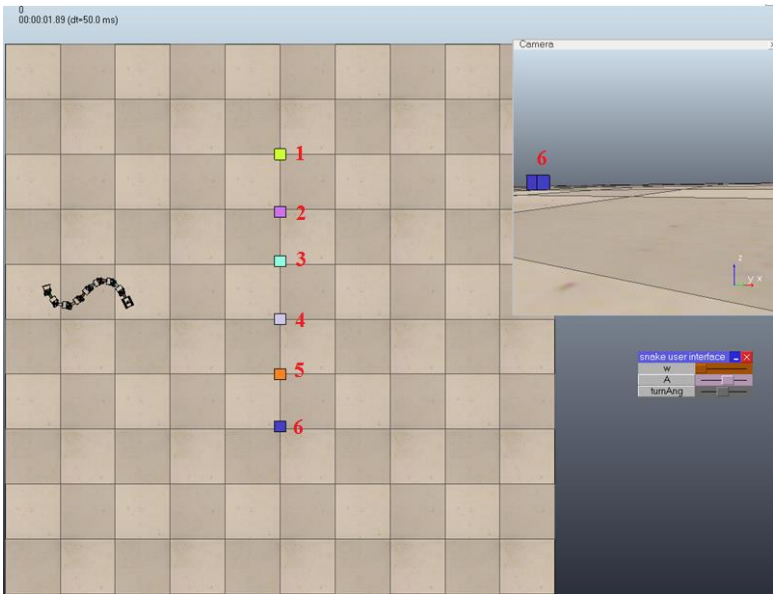

(c) t = π

Figure 4.6 The camera sight of snake robot when moving forward
(continue on next page)

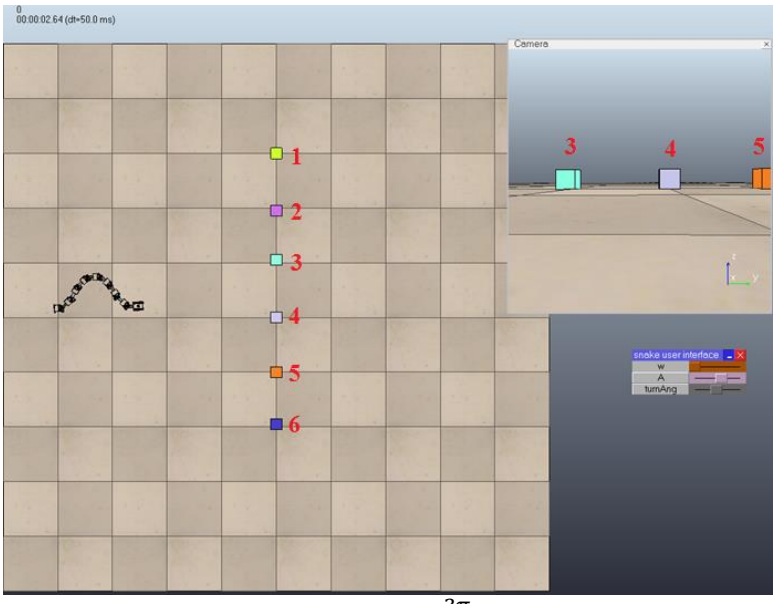

(d) t = $\frac{3\pi}{2}$

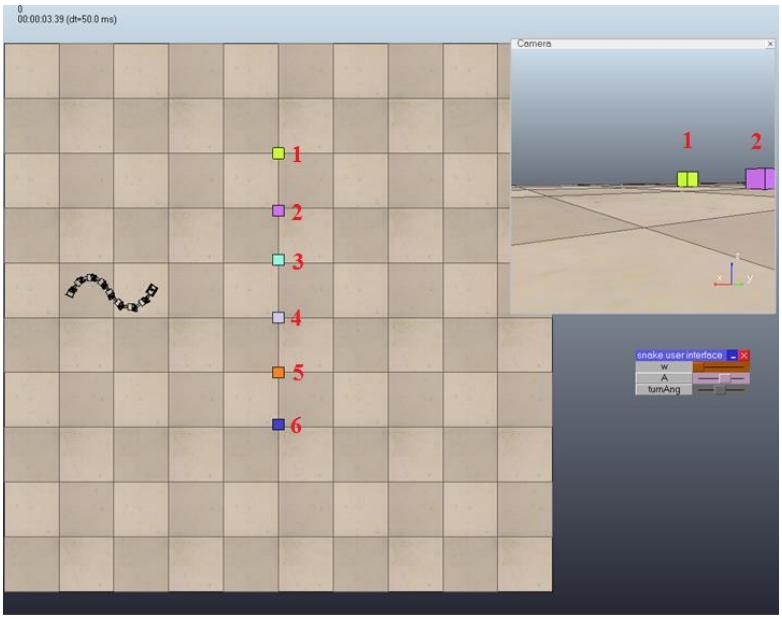

(e) t = 2π

Figure 4.6 The camera sight of snake robot when moving forward

Figure 4.7 indicates the angular velocity of the snake robot head. It shows that the maximum head angular velocity is about 125 when the snake robot is performing steady serpentine locomotion.

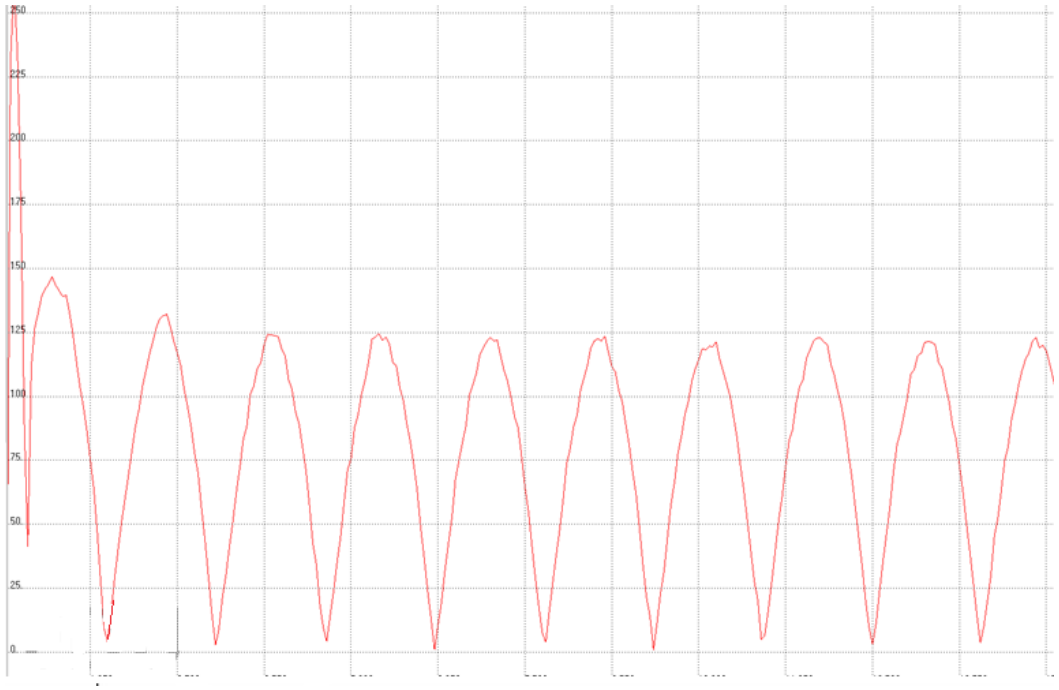

Figure 4.7 The snake robot head angular velocity

4.3 Modification

The camera on the snake robot head takes the video images of the front view of the robot along the camera sight direction. In order to facilitate the remote control operator, who controls the snake robot according to the video images feedback from the camera, the camera sight direction should align with the moving direction.

The snake robot head will be modified so that its orientation aligns with the body moving direction as it travels along the serpenoid curve as shown in Figure 4.8.

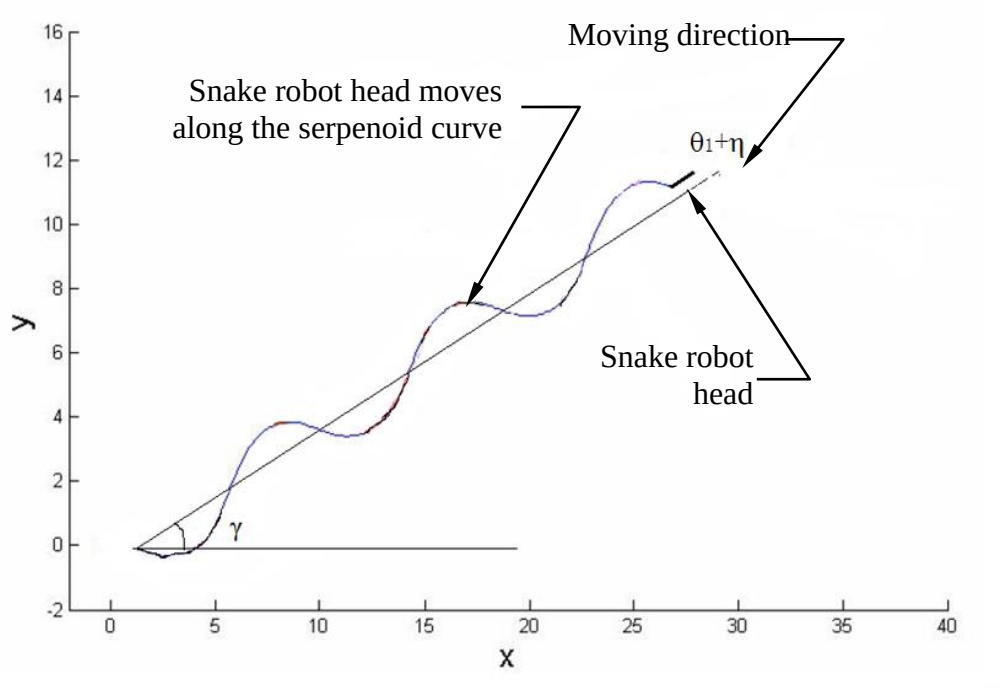

Figure 4.8 Camera sight direction after modification

The camera sight direction is modified so that an angle η is added to the $\theta_1$and the camera sight direction aligns with moving direction. Hence:

$$\theta_1 + \eta = \gamma \tag{4.2}$$

This ensures that the camera sight direction is parallel to the moving direction most of the time.

From the equation (3.31), $\theta_i = a\cos\left(\frac{i}{n}\cdot\frac{2K_n\pi}{L}\right) + \frac{i}{n}c = a\cos(k\beta) + k\gamma$ yieldsθ_1=$a\cos(\beta) + \gamma$.

As mentioned in previous chapter, the snake robot head is oscillating during the motion. Rewriting the θ_1 in time dominion $\theta_1(t)$ gives

$$\theta_1(t) = (g * a)\cos(\omega t + h\beta) + \gamma \tag{4.3}$$

From equation (4.2):

$$\eta(t) = -(\theta_1(t) - \gamma) = -\big((g * a)\cos(\omega t + h\beta) + \gamma - \gamma\big)$$

$$= -(g * a)\cos(\omega t + h\beta) \qquad (4.4)$$

This modified head angle ($\theta_1 + \eta$) is added to the relative angle in the first joint $\emptyset_1(t)$ to revise the headorientation. In the transformation from equation (3.32) to (3.33), only the trend including amplitude α and phase difference β of the sinusoidal manner is adopted. In order to generate the modified head angle so that it couples the relative angle to keep the same trend. A set of coupling factors (g, h) is introduced and shown in equation (4.5).

The first joint relative angle equation is

$$\emptyset_1(t) = \alpha \sin(\omega t + (i-1)\beta) + \gamma - (g * a)\cos(\omega t + h\beta) \qquad (4.5)$$

This thesis will use the experimental method in the simulation to find the coupling factors (g, h). In the simulation and implementation, a specific serpenoid curve will choose the parameters (α, β), then various sets of (f, g) are tried to optimize the angular velocity $\dot{\theta_1}(t)$of the first segment.

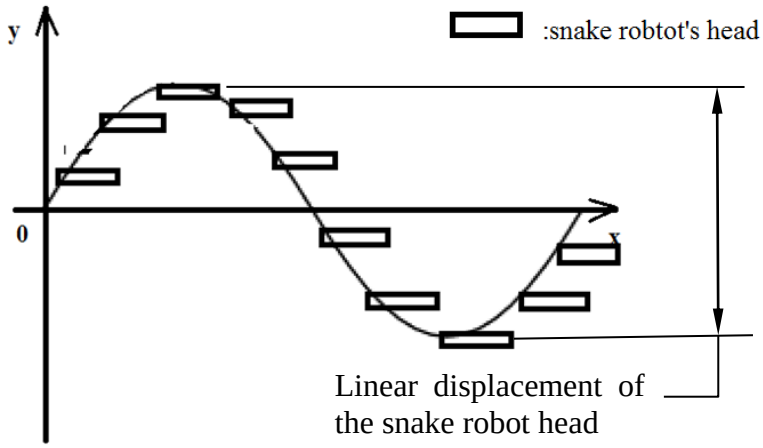

Figure 4.9 The snake robot head direction after modification in a motion cycle

Figure 4.9 shows the head orientation is heading forward all the time during a motion cycle if the coupling factors match a particular serpenoid motion(α, β) in real time. Hence, there is only liner displacement of the snake robot head perpendicular to the moving direction without any angular rotation about its centre of gravity. This indicates that the optimal coupling factors result in the minimum angular velocity $\dot{\theta}_1(t)$ of the head.

The ranges of the factors (g, h) are determined by the parameters of a serpenoid motion (α, β).

From the equation (4.13), the absolute amplitude of the first joint relative angle is:

$$A = \sqrt{\alpha^2 + (g * a)^2} \tag{4.6}$$

which is limited by the rotational range of a servo motor, and the maximum angle is 90^o, hence

$$g \in \left[0, \frac{\sqrt{(\frac{\pi}{2})^2 - \alpha^2}}{a}\right] \tag{4.7}$$

From the principle of $\cos(x + 2\pi) = \cos(x)$, The range of g is:

$$h \in \left[0, \ \frac{2\pi}{\beta}\right] \tag{4.8}$$

The optimal coupling factor is found by following procedures:

1. In the simulation, set h=0, then increases g from 0 to $\frac{\sqrt{\frac{\pi^2}{2} - \alpha^2}}{a}$ by a step of 0.1 to find the value of g_1 which has the minimum head angular velocity $\dot{\theta_1}(t)$.
2. With the best g_1 found in (1), increase the value of h from 0 to $\frac{2\pi}{\beta}$ by a step of 0.1 to find the value h_1 which yields the minimum head angular velocity $\dot{\theta_1}(t)$.
3. A small modification of (g_1, h_1) in its close range $(g_1 \pm 0.1, h_1 \pm 0.1)$ with a step of 0.01. Iterate and follow the trend of increase and degrease of head angular velocity $\dot{\theta_1}(t)$ until the final coupling factor in 0.01 resolution (g_m, h_m) is found.

This modification only optimizes the head orientation to align with the moving direction; the robot head still has the linear displacement perpendicular to the moving direction and this displacement depends upon the amplitude of the serpenoid curve during serpentine locomotion.

4.4 Simulation of the modification

In the section 4.3, the modification of snake robot head is presented. The experimental method to find the coupling factor (g_m, h_m) is accomplished in this

part. From the equation (4.7) and (4.8), substituting a=$\frac{\pi}{3}$ and $\beta = \frac{2\pi}{9}$ yields the ranges of g and h such that g$\in [0, 1.6]$, h$\in [0, 9]$.

Figure 4.10 shows variation of snake robot head angular velocity against the value of g when h = 0. The minimum value of head angular velocity happens at g=0.9 (or g_1= 0.9).

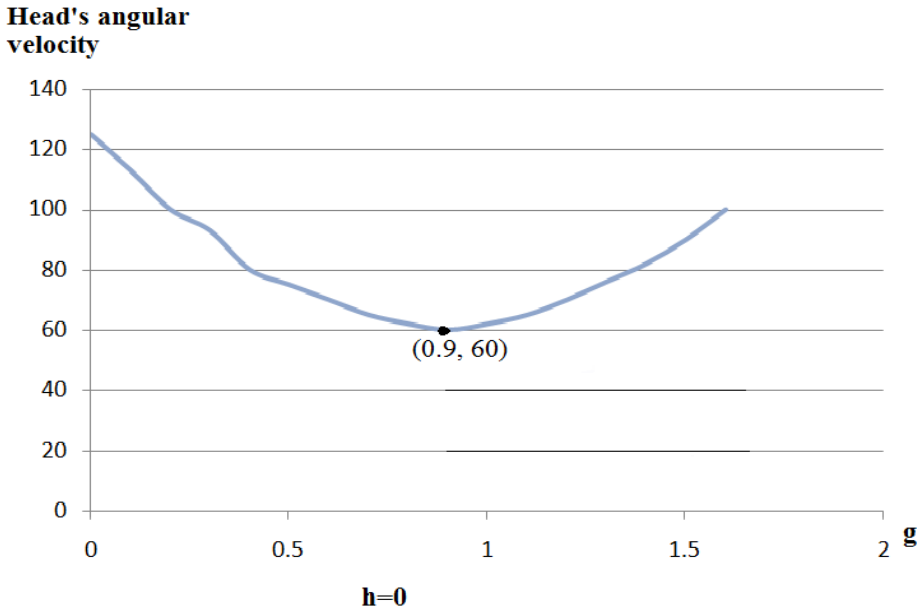

Figure 4.10 Finding g_1 when h=0

Figure 4.11 shows the minimum value of head angular velocity at h=8.2 (h_1=8.2) when g (=g_1) =0.9.

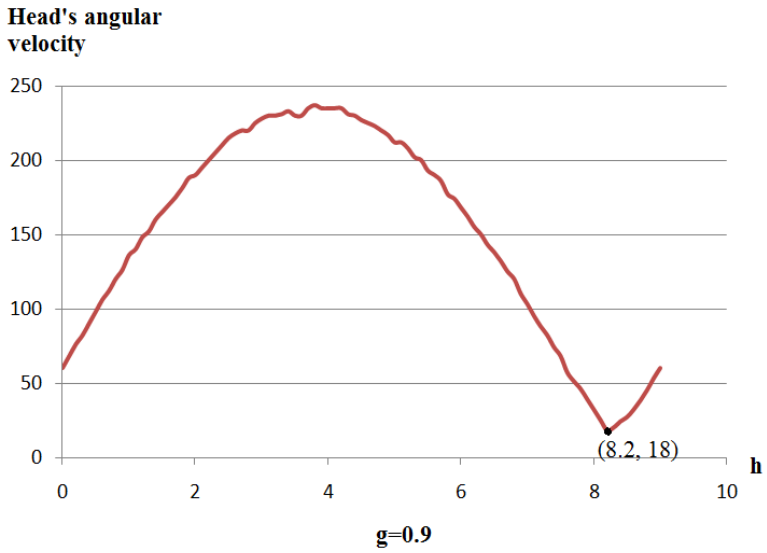

Figure 4.11 Finding h_1 when g=0.9

Based on the values of g and h obtained, a range of coupling factorsof (0.9±0.1, 8.2±0.1) is established. The same procedures of (1) and (2) are repeated to find (g_m , h_m) which yields minimum head velocity. Finally the coupling factors are (1.0, 8.28), and the angular velocity after modification is presented in figure 4.12. The maximum value of the head velocity is 9.1 which is greatly reduced as the value before the modification is 125.

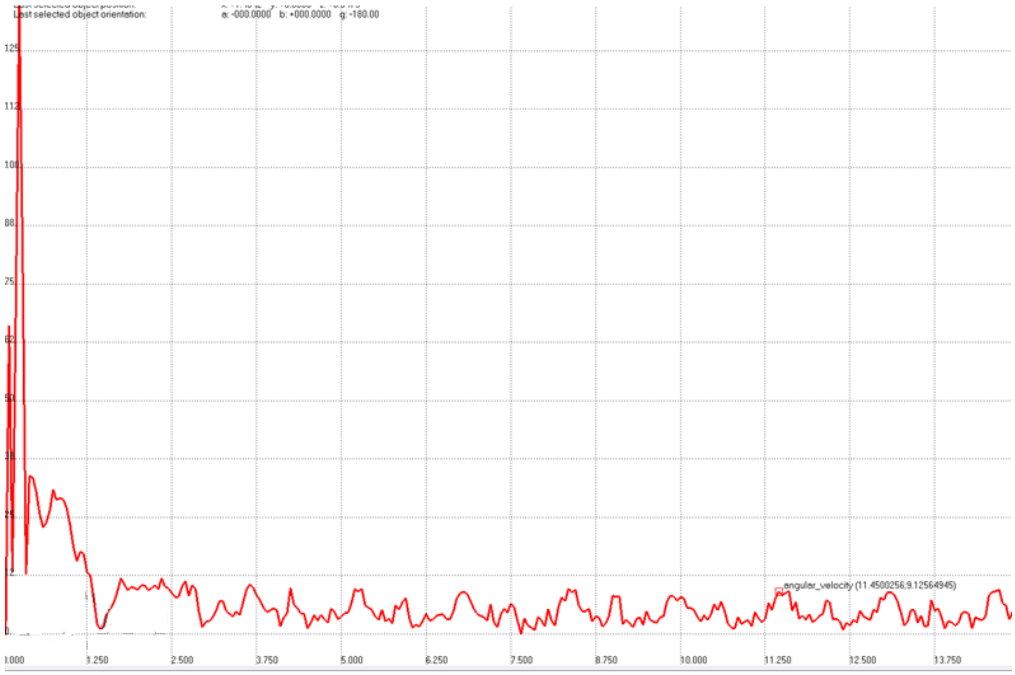

Figure 4.12 The angular velocity of snake robot head after modification

4.5 Modification result

With the coupling factors and the modified angle added in the first joint relative angle, the relative head angle at the joint is

$$\emptyset_1(t) = 41.04 \sin\left(-\omega t + (i-1)\frac{2\pi}{9}\right) + \gamma - (1 \times \frac{\pi}{3}) \cos\left(-\omega t + 8.28 \times \frac{2\pi}{9}\right)$$

This part shows the snake robot shape during locomotion as well as the camera sight. Additionally, decreasing amplitude of snake robot also reduces the linear displacement perpendicular to the moving direction. Hence, the camera view is relatively more stable.

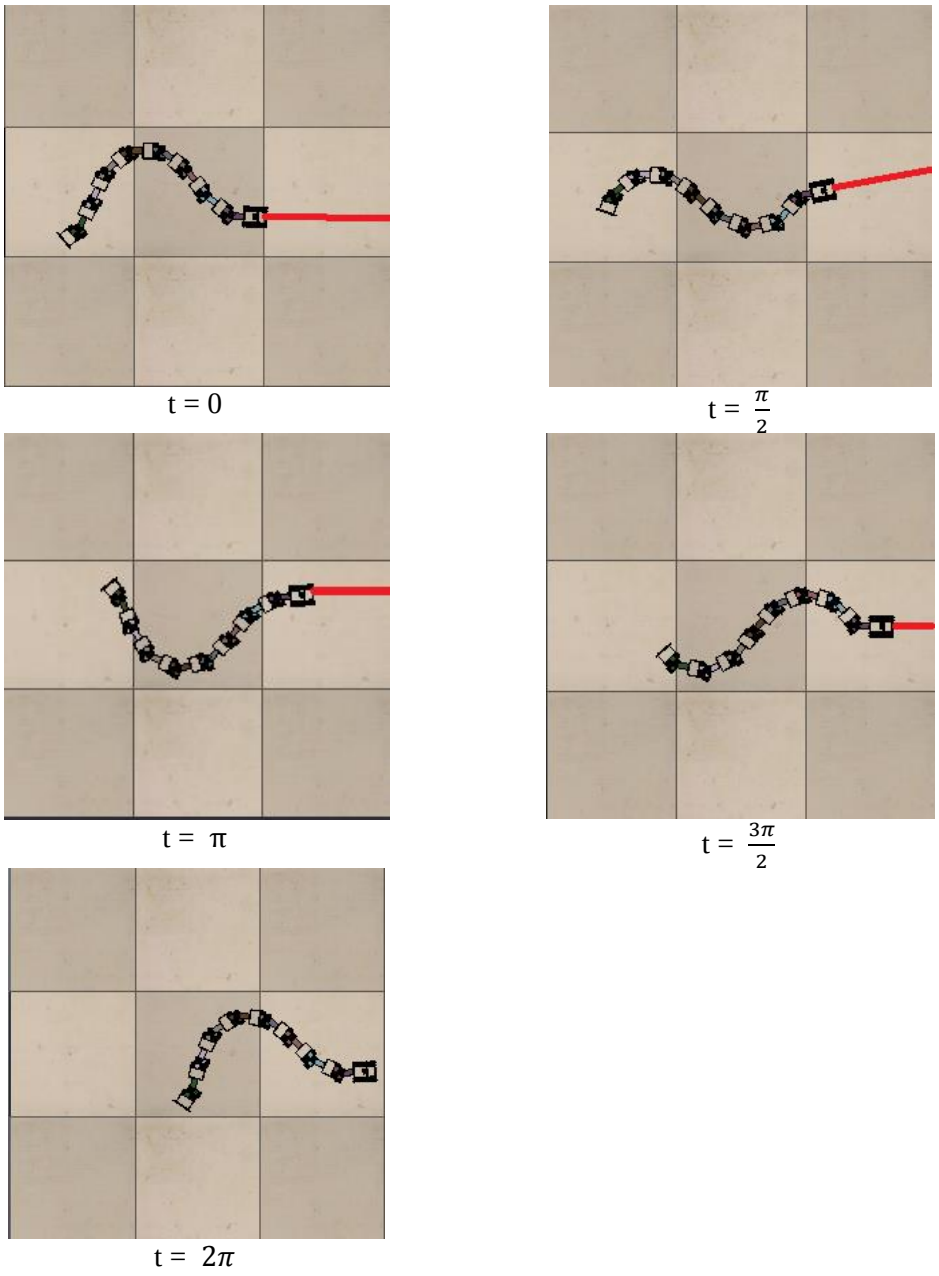

Figure 4.13 Snake robot shape after modification in one moving cycle

The figure 4.13 shows the shape of snake robot in one moving cycle after the head modification. The snake robot head is approximately "looking forward" all the time when the snake is simulated to move forward.

Figure 4.14 presents the camera sight of snake robot during locomotion. From the 4.14 (a) to 4.14 (e), all the camera sights include the cube 3, which indicates that the swing of camera view is not large and the moving direction of snake robot can

be recognized from the camera view. The camera covers 3 cubes (cube 2, 3 and 4) in the whole moving cycle.

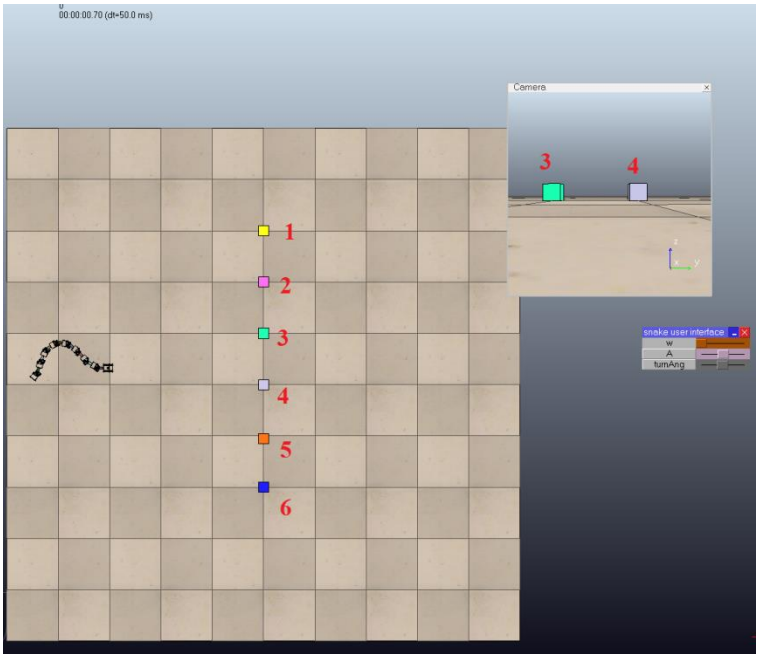

(a) t = 0

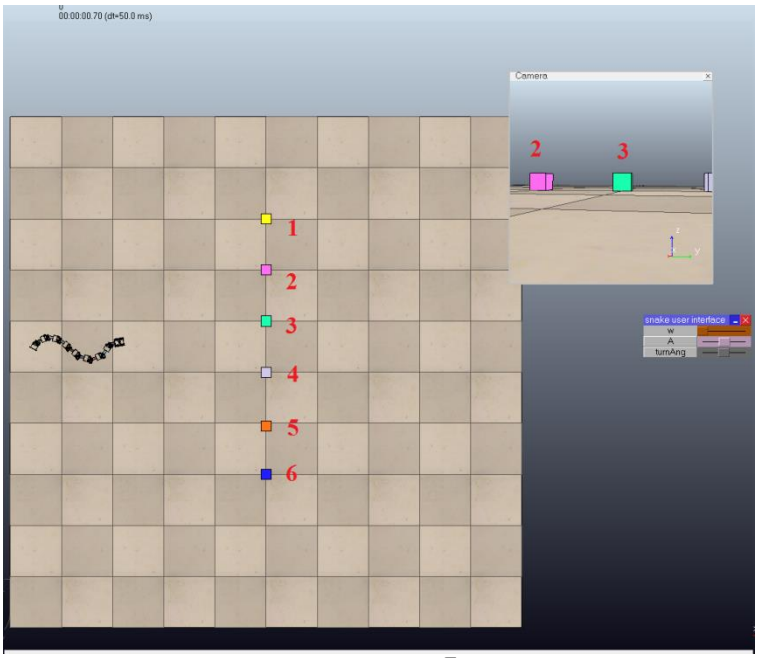

(b) t = $\frac{\pi}{2}$

Figure 4.14 Camera sight of snake robot after modification
(continue on next page)

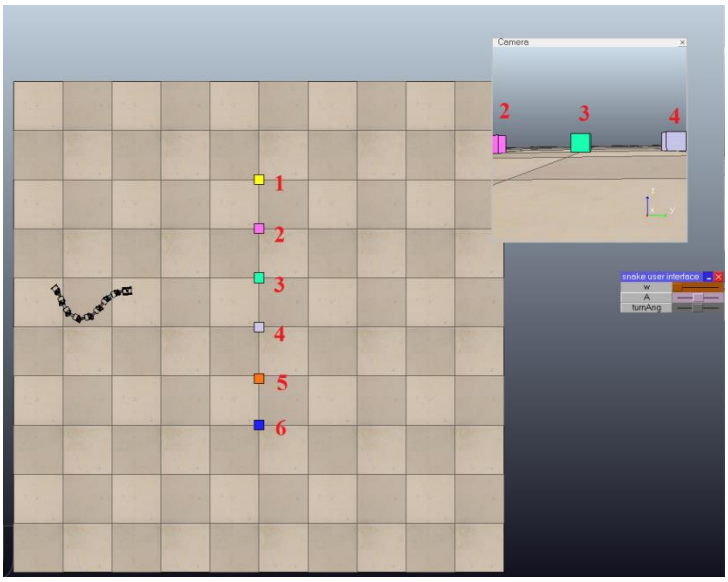

(c) t = π

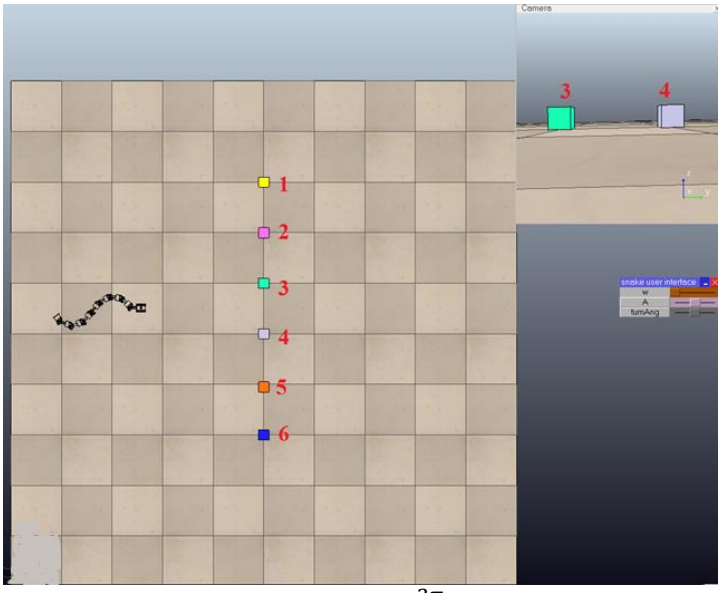

(d) t = $\frac{3\pi}{2}$

Figure 4.14 Camera sight of snake robot after modification
(continue on next page)

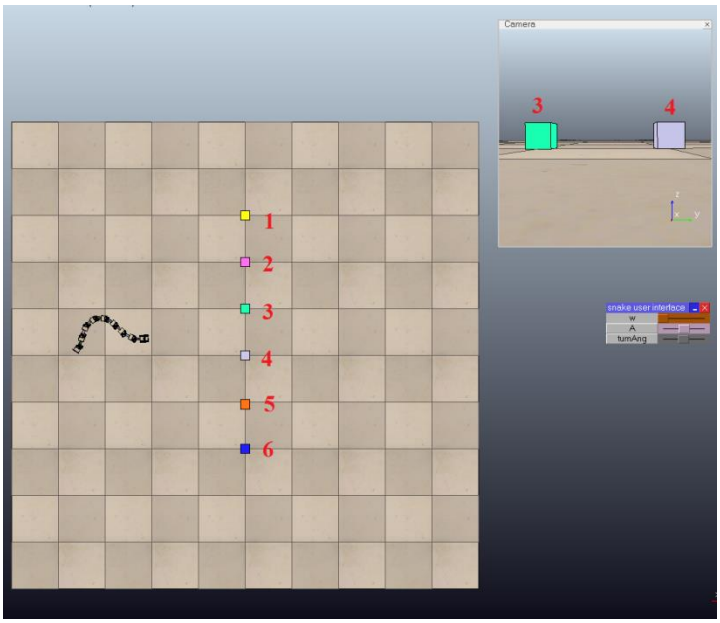

(e) t = 2π

Figure 4.14 Camera sight of snake robot after modification

Figure 4.15 shows the effect on the linear displacement of the snake robot head when the amplitude α decreases to 30^{o} from 45^{o} , the shape of snake robot becomes flatter, but the swing of camera sight does not reduce a lot due to the perspective projection of camera is relative large. The camera sight of Figure 4.14 and Figure 4.15 both include cube 3 and cube 4 in all the motion time which show that the modification is suitable for direction recognition.

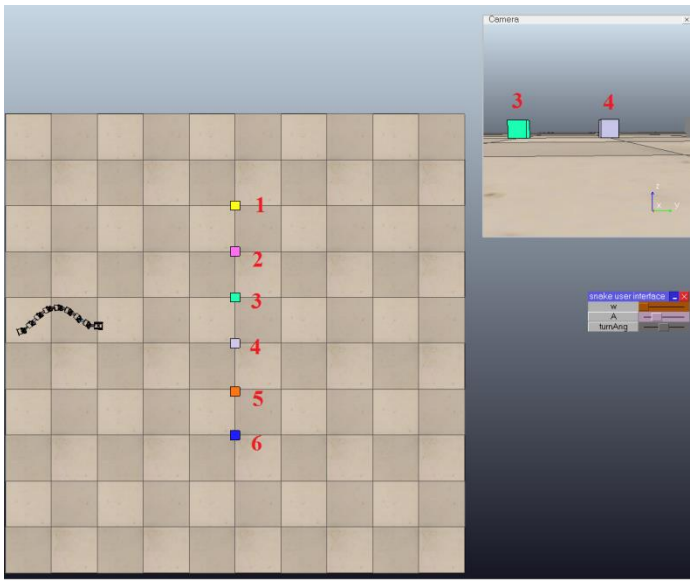

(a) t = 0

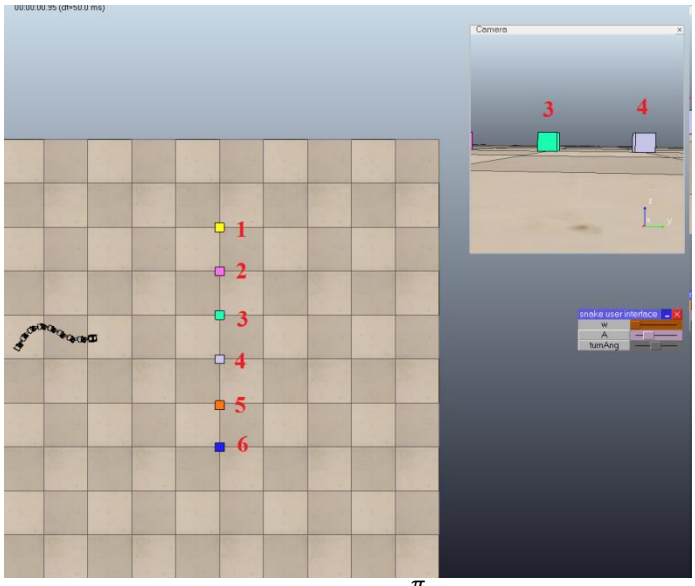

(b) t = $\frac{\pi}{2}$

Figure 4.15 Snake robot with decrease of amplitude
(continue on next page)

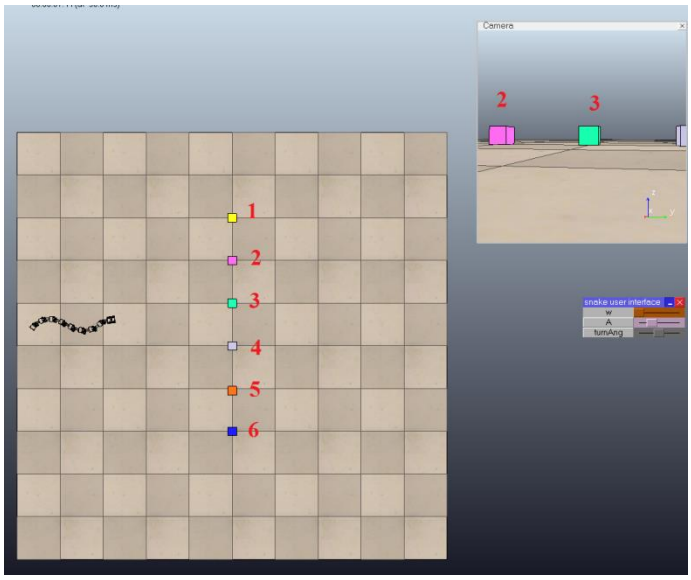

(c) t = π

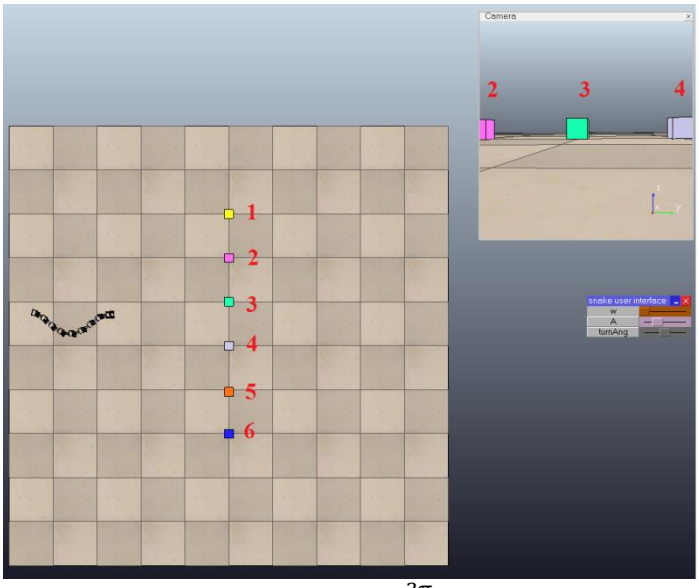

(d) t = $\frac{3\pi}{2}$

Figure 4.15 Snake robot with decrease of amplitude
(continue on next page)

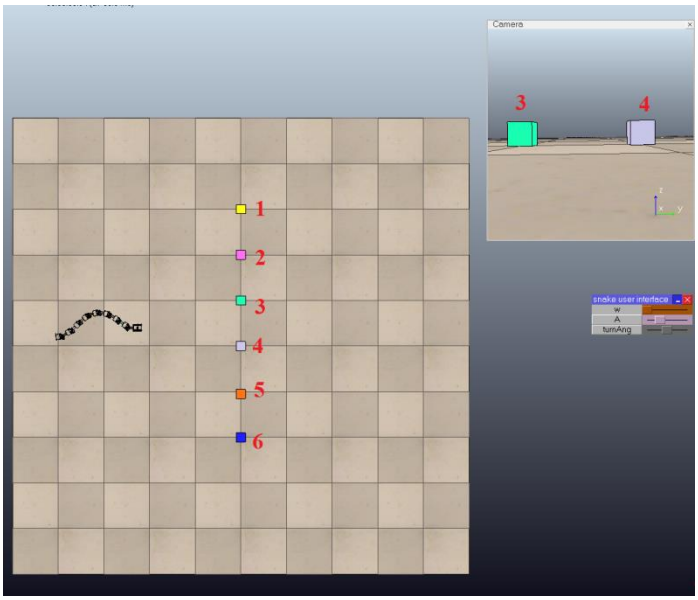

(e) t = 2π

Figure 4.15 Snake robot with decrease of amplitude

Chapter 5. Implementation

5.1 Hardware and software

In the previous chapters, the simulation and the modification on V-REP have been accomplished. This chapter will discuss the implementation of the snake robot. The snake robot contains 16 servo motors which control the vertical and horizontal movement in each joint respectively. After assembling the length is about 1 meter in straight as in Figure 5.1.

Figure 5.1 Implantation of snake robot

As indicated in Figure 5.2, each joint has two servo motors which are fixed on the two servo brackets as shown in Figure 5.2(a). The joints are linked by two U-shape brackets arranged perpendicularly. These U-shape brackets can be rotated by the servo motors. In this way, the snake robot has 16 degrees of freedom. All the motors can rotate 180^{o} degrees, 90^{o} in both directions. Besides, at the bottom of each joint, a passive wheel is attached. The wheels can decrease the friction with ground and prevent the snake from slipping so that the kinematics constraint $\dot{x}_i \sin\theta_i - \dot{y}_i \cos\theta_i = 0$ (equation (3.3)) is implemented.

(a) Two servo brackets with two servo motors

(b) U-shape brackets linking the joints

Figure 5.2 Configuration of each segment

There is a gamepad module at the head of snake as shown in figure 5.3(a). It provides settings and simple position obtaining commands with 12 buttons. A wireless gamepad as shown in Figure 5.3(b) can be connected to the module and be used to control the snake moving direction.

(a) A gamepad module

(b) A wireless gamepad

Figure 5.3 The wireless gamepad and module

The chargeable battery pack used for the snake robot is 10.8 volts and 750mAh which can be used continuously for nearly 30 minutes. And the charger together with the battery pack needs 2 hours to charge it full.

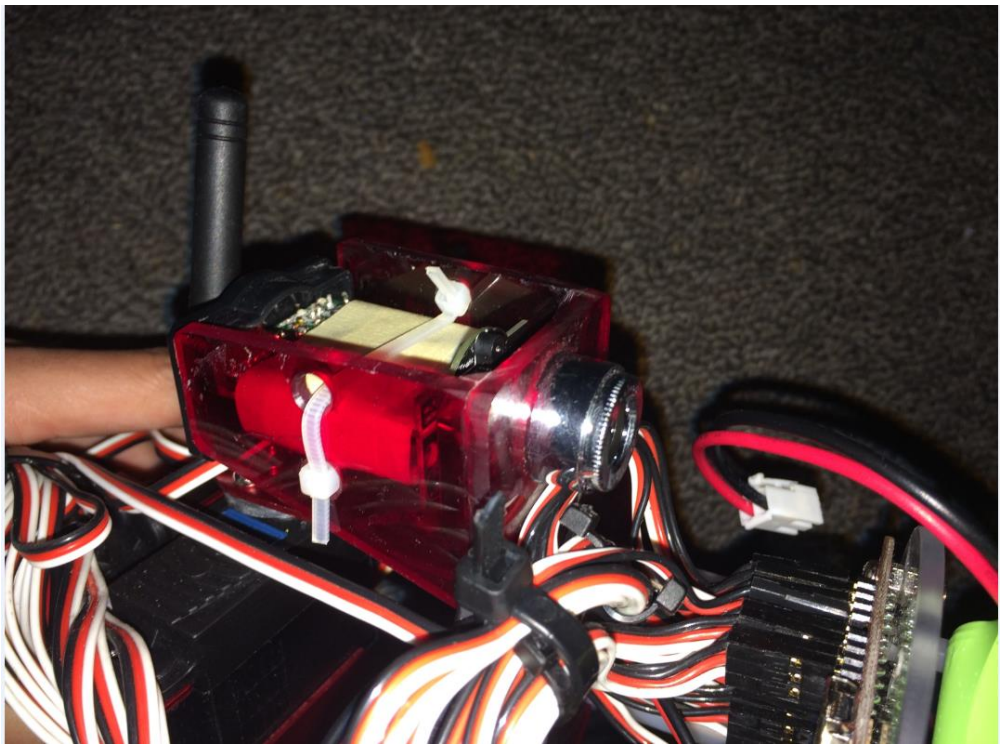

Figure 5.4 The wireless camera

Figure 5.4 presents the wireless camera attached on the snake robot head. With the USB wireless receiver, video images shot by camera is shown on a laptop screen.

Figure 5.5 presents the video images received on computer when snake is moving. The snake robot is controlled to move on a bench by the gamepad based on the video image from the camera (the operator does not look at the snake robot when he controls the robot).Some items are located in front of the snake robot, which are “seen” by the snake so that the images are transmitted to the laptop. From Figure 5.5 (a) and (b), those background items are seen on the screen of the laptop and are out of sight when the snake turns around as shown in Figure 5.5(c) and (d).

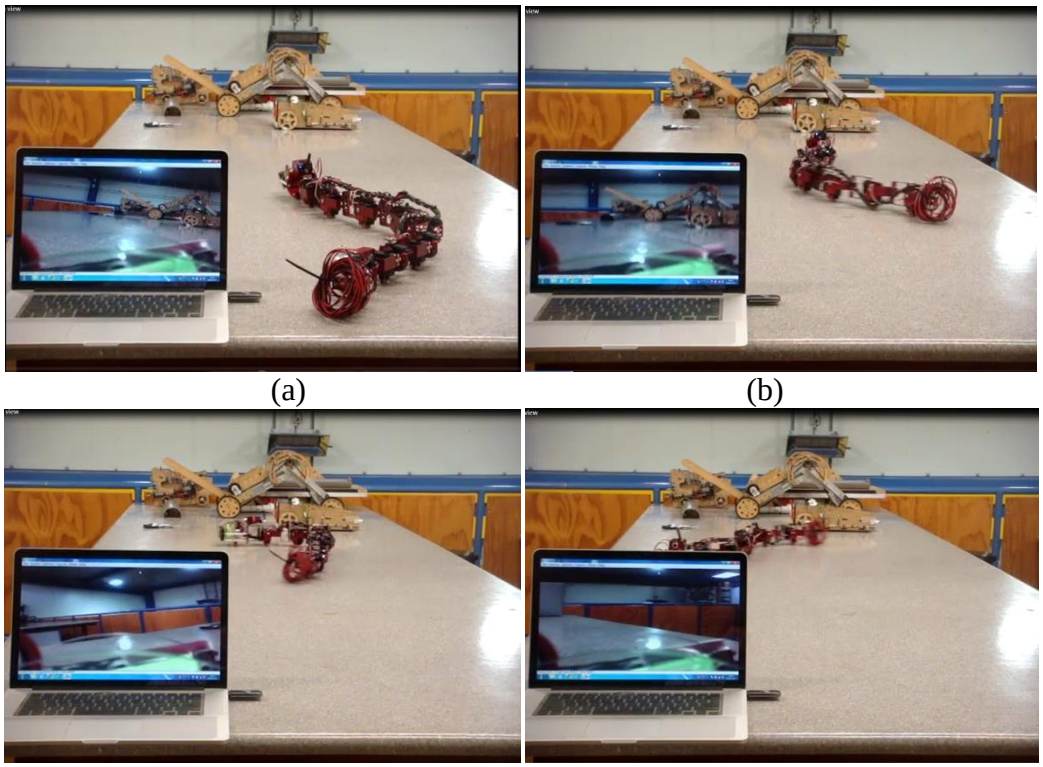

(a) (b)

(c) (d)

Figure 5.5 Camera view when moving

The software part employed the equation deduced in chapter 4 with the amplitude set as 30^{o}. Some key program statements of the code in the microcontroller are present in appendix B.

5.2 Result of implementation

This part is the result obtained from the implementation. The snake robot is assumed to move on a flat surface under the remote control. Pictures will be taken every 0.5 second to show the snake shape and the movement. Two cans of “Coke” and “Sprite” with a distance of 0.5m apart are located in front of the snake robot. Figure 5.6 shows the initial position and body shape of snake robot. The snake robot is controlled to move forward and modify its moving direction through the

wireless gamepad under the direction recognized from camera view. Finally, the snake robot is assumed to reach the can of “Sprite” on the left hand side.

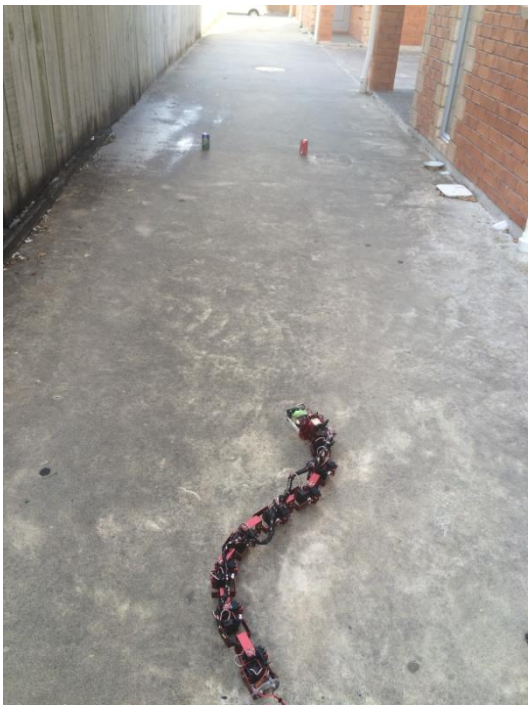

Figure 5.6 The initial locations of the snake and the cans

Figure 5.7 shows the video images captured by the wireless camera installed on the snake robot head. These images are transmitted to the laptop of the operator who does not see the snake robot. This operator controls the snake robot using the gamepad based on the laptop screen. At the beginning (t = 0), both cans are captured by the camera view. The snake robot moves along the line of sight which is its camera sight direction. As the small linear displacement of the snake robot head perpendicular to the moving direction, the images shift a bit from t = 0 to t = 6s. After 6 seconds, the snake robot has been advanced almost half of its journey and starts changing its head orientation heading towards the can of “sprite”. Hence, only the can of “Sprite” is seen on the laptop screen after 6 seconds and the snake robot arrives at the destination (can of “Sprite”) at time t = 11s.

t = 0s

t = 1s

t = 2s

t = 3s

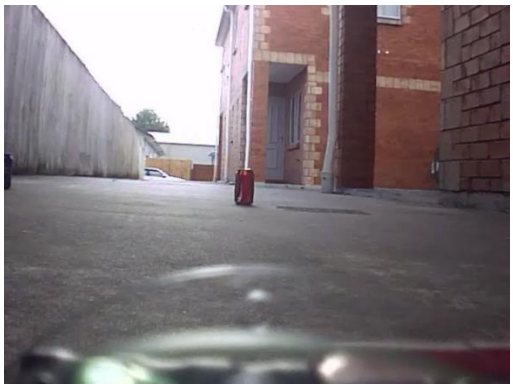

t = 4s

t = 5s

Figure 5.7 The video images captured by the camera on the snake robot head (continue on next page)

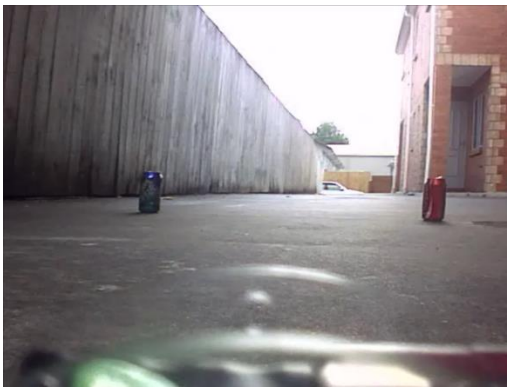

t = 6s

t = 7s

t = 8s

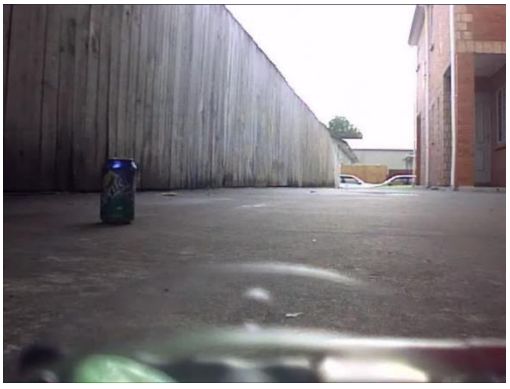

t = 9s

t = 10s

t = 11s

Figure 5.7 The video images captured by the camera on the snake robot head.

Figure 5.8 shows the how the snake robot moves in the field. It has a quit consistent head orientation in the first 6 seconds heading toward the front. The line of sight is basically pointing to the can of “Coke”. It also corresponds to the video image shown in Figure 5.7 in the first 6 seconds that the can of “Coke” is

almost at the centre of camera view. At the seventh second, the line of sight shown in Figure 5.8 points to the can of “Sprite” and eventually reaches there at eleventh second. Consequently, the can of “Sprite” becomes the main object in Figure 5.7 after the seventh second.

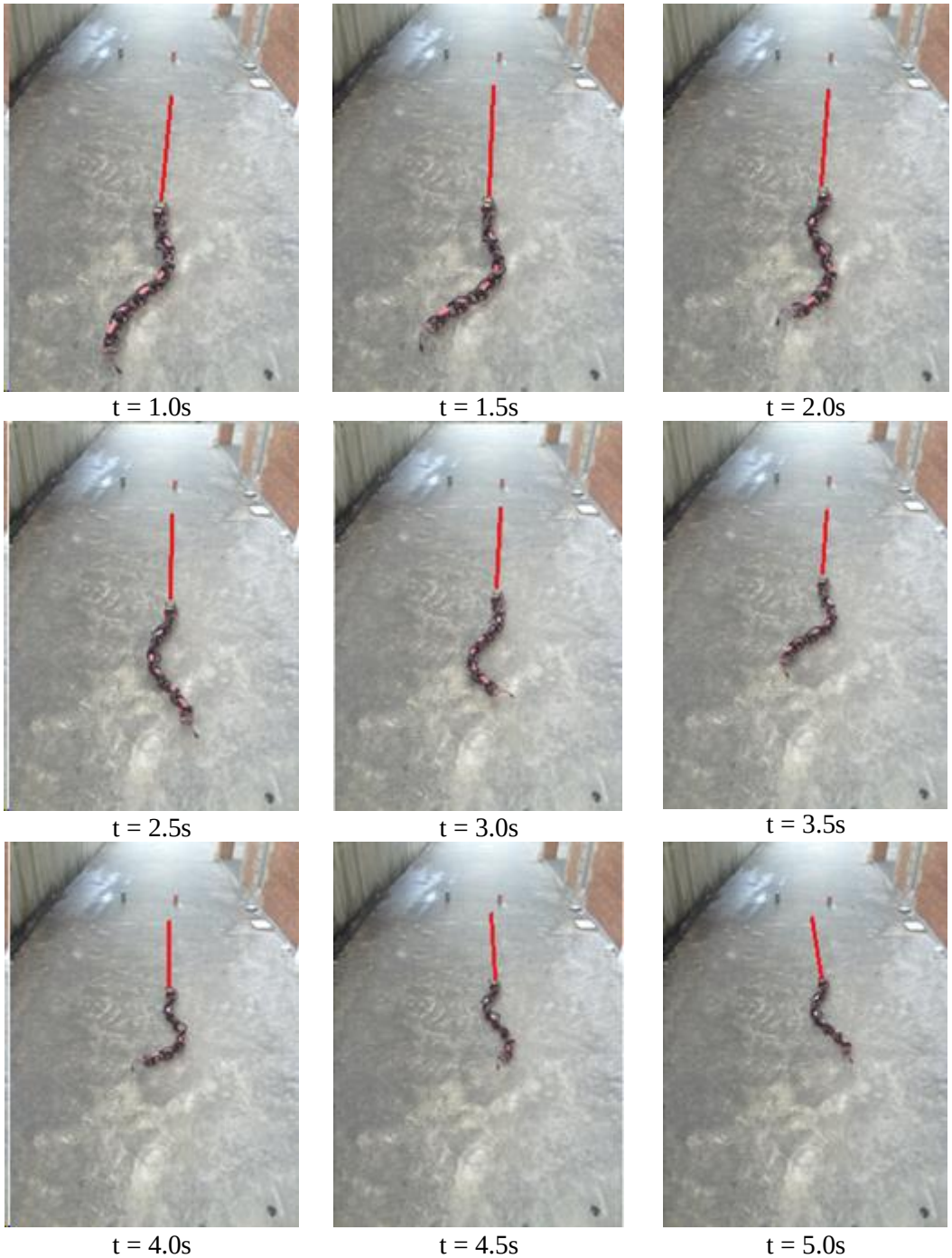

Figure 5.8 The shape of snake robot during moving (continue on next page)

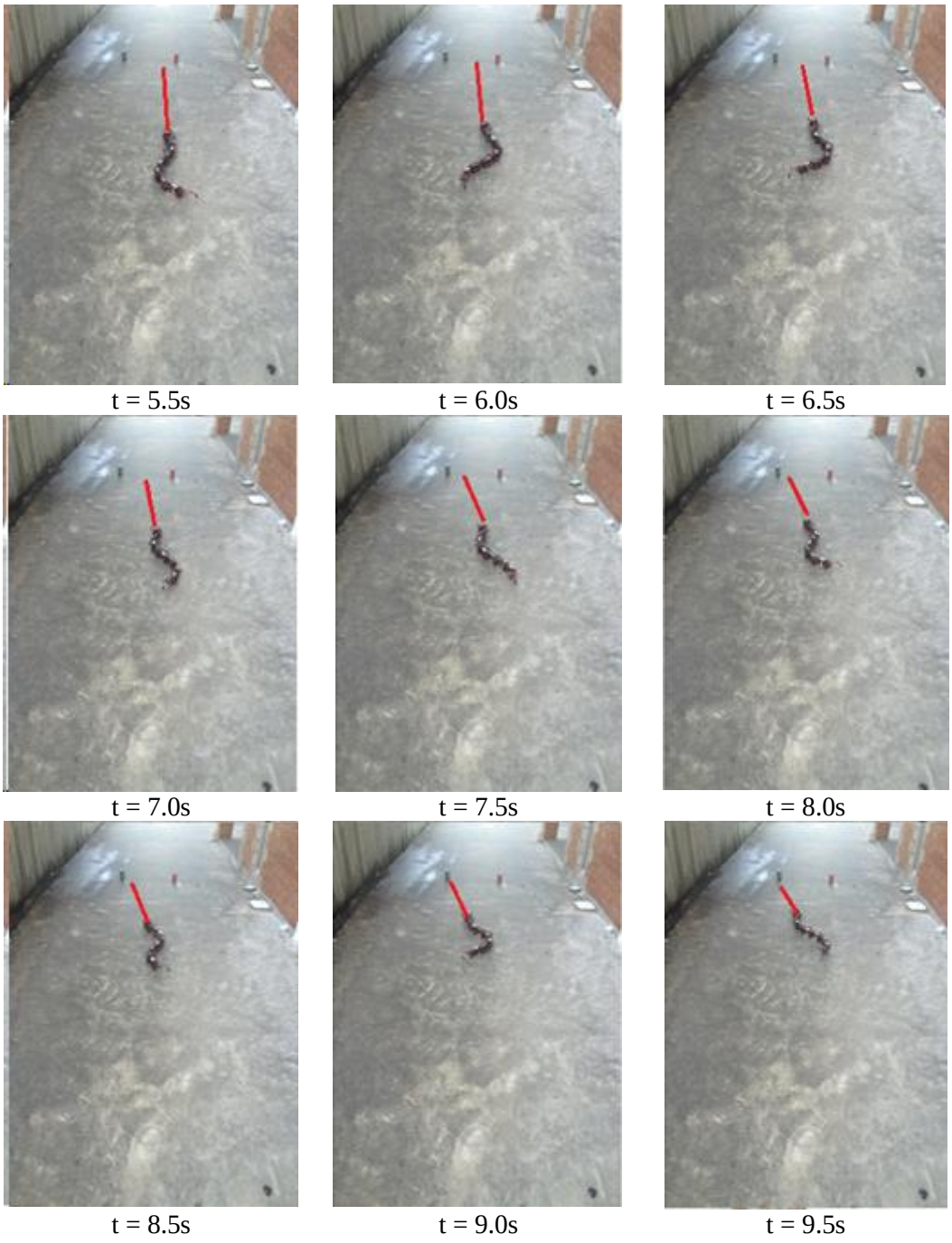

Figure 5.8 The shape of snake robot during moving (continue on next page)

t = 10s t = 10.5s t = 11s

Figure 5.8 The shape of snake robot during moving

Comparing with the simulation results, the implementation results are similar, only with smaller amplitude; the camera sight swing is smaller as well. And the basic goal of controlling the snake robot locomotion according to the video images from a camera is achieved.

Chapter 6. Discussion

In this chapter, some findings and issues during the research will be discussed. The content includes limitations, kinematics, controls and implementation issues. Furthermore, the caterpillar locomotion is also introduced.

6.1 Different kinematics limitation

In Chapter 3, it is assumed that no slipping happens in the normal direction to the body segment such that $\dot{x}_i \sin\theta_i - \dot{y}_i \cos\theta_i = 0$. This is implemented by installing a single wheel in each segment so that the body segment only move along the tangential direction of the body segment. However, this assumption does not hold all time and the snake robot slips inward and outward along the normal direction of the body segment. This happens seriously especially when the ground friction is relatively large such as locomotion on a carpet.

In fact, a wheeled snake robot definitely has slipping along the normal direction of the segment (Ma, 2001) as the coefficient of friction along the normal direction of the segment is not zero. It is just ignored due to the relatively large coefficient of friction along the tangential direction.

6.2 Limitation of the modification

In the snake robot head modification, the camera is installed on the first segment of the snake robot with optimal absolute joint angle so that the camera sight direction is constantly parallel to the moving direction. A pair of couple factors (g, h) is used to achieve the purple of aligning the snake robot head with the moving direction. In the procedures to find the coupling factor (g, h), only the trends of increase and decrease are followed to get the value with the minimum head angular velocity. Comparing with the complete coverage of all the points in the ranges of g and h, using the simulation to compute the coupling factor greatly reduce the computation expenses. Furthermore, its implementation is much simpler than optimization method such as genetic algorithm (Hasanzadeh & Toothoonchi, 2008). Whereas, the result can be more accurate if all the values of (f, g) are covered and the snake robot head oscillation can be decreased a bit more.

On the other hand, only the direction of snake robot head is modified in this approach. The camera still has the linear displacement normal to the moving direction with a fixed orientation. The video images received by the camera are still shifting according to the amplitude of snake robot serpentine locomotion. However, this does not actually affect the purpose of remotely controlling the snake robot. In fact, this is similar to the head movement of a biological snake (National Science Foundation, 2015). Forcing the head remains along the moving direction (Sergiienko & Chen, 2014) distorts the body shape of the snake robot and consequently affects the locomotion speed.

6.3 The control strategy

In the chapter 2, three approaches of control strategies are discussed, which are based on the trajectory, torque and central pattern generator respectively. The trajectory based control is adopted in this research. This method mainly analyses the motion curve of a biological snake, then combines with the kinematics and dynamics calculation to deduce the relative angle for all the joints. The advantage of the trajectory based control is its ease of achieve and more flexible for the controlling code implementation. However, this approach only suits for the motion with regular pattern such the serpentine motion. In the search and rescue situation, the irregular surfaces require the snake robot to include various locomotion patterns to accomplish the complicated situation. Hence, the central pattern generator (CPG) control is more suitable. The CPG enables each motor to be independent and the relative angles for all the joints are calculated based on the information and data received by the sensors as a close-loop feedback control.

6.4 Caterpillar locomotion

The thesis mainly discusses the serpentine motion and the modification of the snake head orientation. Meanwhile, the caterpillar motion is also studied during the research and the following paragraphs will have a brief introduction. The caterpillar motion is also called the pitch-patch motion. It has a similar mathematic model as the serpentine motion. It just performs the serpentine locomotion in the x-z plane instead of the x-y plane. The relative angle is given as (JUAN GONZÁLEZ GÓMEZ, 2008)

$$\emptyset_i(\phi) = 2\alpha \sin(\frac{\pi k}{M}) \sin(\phi + \frac{2\pi k}{M}[(i-1) + \frac{d_0}{d}]) \quad (6.1)$$

where$\phi_t = \frac{2\pi}{T}t$

The table below describe the meaning of each parameter, as well as its range.

Table 6.1 Definitions of parameters in caterpillar motion equation

Parameter	**Description**	**Range**
k	Number of undulations	$k \geq 1$
α	Winding angle	$\alpha \in [0, 120]$
M	Number of articulations	$M \geq 2$
d	Distance between joints	$d > 0$
d_0	Left segment of the module	$d_0 > 0$
ϕ	Phase	$\phi \in [-180, 180]$
i	Joint number	$i \in \{1,M\}$

Winding angle is defined as the angle that forms the tangent that passes through the point of the curve start point.

The equation of the relative angle at the joint for serpentine motion and caterpillar motion are very similar, only the definitions of parameters are different. The patch-pitch equation has an additional parameter$\frac{d_0}{d}$ inside the sine curve.

The simulation of caterpillar locomotion is also conducted in V-REP. As this motion is useful when the robot need to climb over the obstacles, the simulation focused on the climb ability. The result is shown in Figure 6.1. In Figure 6.1(a), the snake robot is moving toward the step at the right hand side with serpentine locomotion pattern. When it detects the step as shown in Figure 6.1(b), it changes to caterpillar locomotion pattern to climb up the step as depicted in Figure 6.1(c).

The snake robot changes back to the serpentine locomotion pattern once it is on the step as Figure 6.1(d).

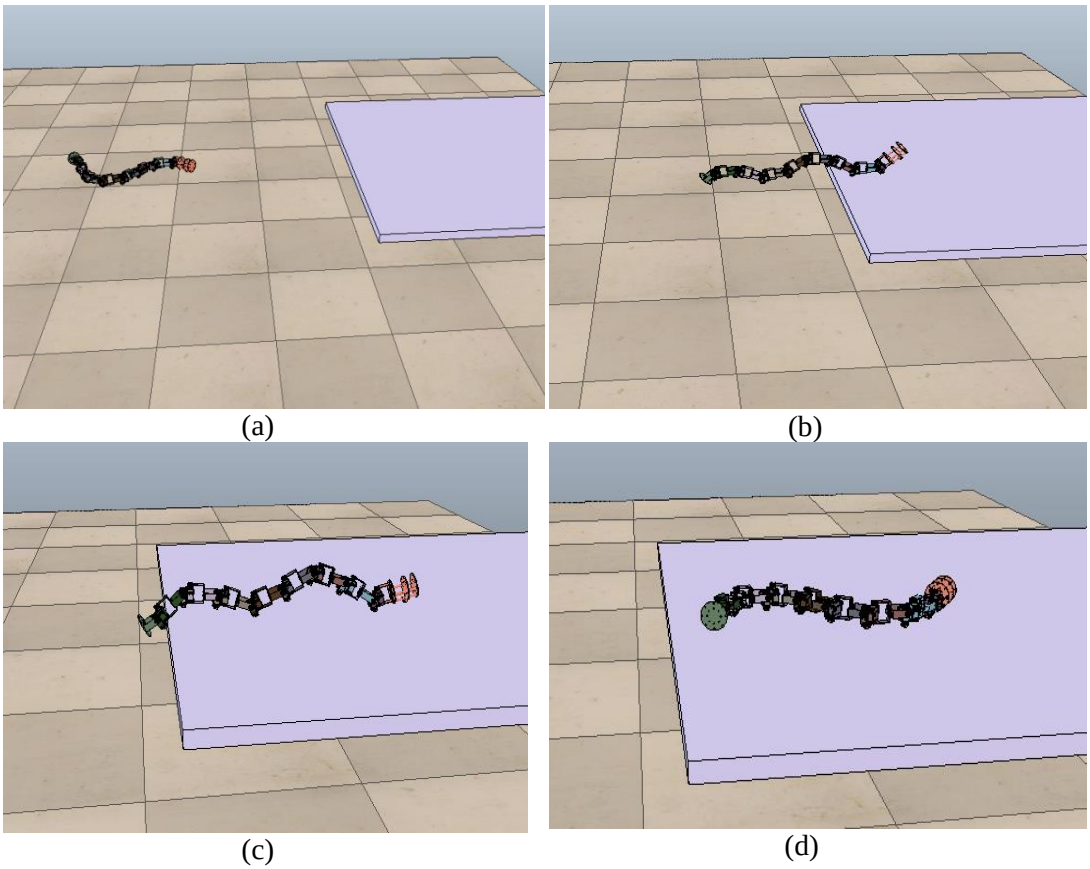

Figure 6.1 The simulation result of climbing up the step by using caterpillar locomotion pattern.

The caterpillar locomotion pattern also possesses the issue of "sight swing" if a camera is installed on the snake robot head. In fact, a similar joint angle modification should also be performed to stabilize the view.

6.5 Implementation issues

Though the snake robot is made and basic movement can be accomplished, various issues arise during the implementation of the snake robot as a research platform. These issues will be addressed in this section.

Firstly, the battery is the most exigent problem that needs to be solved. It costs 2 hours to fully charge the battery, but it can only last for 30 minutes. This performance is not acceptable in the real situation. In fact, at least 2 hours continuous operation is required in the real rescue operations. Hence, a high energy density battery is necessary. Another aspect which affects the operation continuity is the weight of snake robot. The snake robot has an aluminium body frame, which cost a lot of energy for the servo motors to generate a large torque to drive the body during locomotion. This large energy consumption rate seriously affects the operational period of the robot.

A user interface of sliders for the amplitude, moving speed and turn angle is implemented in the simulation software V-REP for controlling the snake robot during simulation. The amplitude of the serpenoid curve can be adjusted by the slider to control the body shape. However, comparing with the actual snake robot, the amplitude of the serpenoid curve cannot be changed during the locomotion. Program needs to be reloaded to microcontroller every time of changing the parameter. So, the program for the microcontroller can be improved so that the amplitude of the serpenoid curve during locomotion is adjustable.

Furthermore, the snake robot cannot move on a rough surface due to the small size of the passive wheels. The diameter of the passive wheel is too small to go over the rough surface such as the carpet. However, large torque servo motors should be put on the snake robot to support a set of large wheels to overcome the resistance force.

The caterpillar motion is a better locomotion to apply on the rough surface. However, the stability of the snake with caterpillar locomotion is inversely

proportional to the snake robot length. Actually, a small up and down movement can be performed by this robot, but it is not the real caterpillar motion. It is the horizontal motion using the serpentine movement with every two adjacent vertical motors exchange their angular position at the same time. It results in the snake robot going up and down and moving forward and backward. Compared with the caterpillar motion, this movement is less efficient and the moving speed is slow. In order to apply the real caterpillar motion, a pair of "feet" should be added on both sides of joints, such as the first generation of ACMR robot to increase its stability.

Chapter 7. Conclusion and future recommendations

7.1 Conclusion

The frequently happened earthquakes in New Zealand and the requirements of help during rescue operations after earthquake drive my research on snake robot. Many degrees of freedom makes the snake robot can apply many kinds of movements. This advantage is significant in search and rescue operations. After analysis the current literatures, the snake robot is a new topic in New Zealand, and a lot of improvements are waited to complete around the world. The theory part and simulation part leading me to the correct direction in the research. By finishing the simulation in the V-REP, we find the motors' equations for the serpentine motion as well as the modification on the head. It gives me an instruction during accomplishing the real snake robot microcontroller. At last the snake robot can move under the control of wireless controller. And the moving speed on flat smooth surface is about 0.75 m/s. A wireless camera is added on the head of snake robot to receive images when snake robot is moving. By modifying the snake robot head, the oscillation of sight decreases a lot compared to the normal serpentine motion.

7.2 Recommendations

In the future, the caterpillar motion mode will be added to the snake robot controller. And by modifying the structure, the snake robot will move more stable. The better battery can make the snake robot with a long time working ability. In addition, there is a great necessity to cover the snake robot with a water-repellent case. The working environment in the real situation is complicated, a water-repellent case ensures the snake robot can move over some water surfaces or even move in the water.

Besides, other kinds of motion should also be researched to deal with the complex surroundings. The CPG controlling strategy will be employed in next generation snake robot. The modification of the snake robot head displacement is also in the schedule. Sensors like the GPS sensor and infrared sensor will be attached to make the snake robot with some intelligence. In the future, snake robot can record the route it moved and design the best way to go out itself. Infrared sensor makes sure the snake robot can get images in dark places as well.

Reference

A. Crespi, A. Badertscher, A. Guignard and A.J. Ijspeert, (2004). AmphiBotI : an amphibious snake-like robot. *Robotics and Autonomous Systems*. 50 (4), pp.163-175

CMU Biorobotics Lab, (2014). *Modular Snake Robots*. Retrieved from http://biorobotics.ri.cmu.edu/projects/modsnake/pictures.html (accessed April 2014).

David Rollinson, Kalyan Vasudev Alwala, Nico Zevallos and Howie Choset, (2014). Torque Control Strategies for Snake Robots. *IEEE/RSJ International Conference on Intelligent Robots and Systems*. September 14-18, 2014, Chicago, IL, USA. pp 1093-109

Erkmen Ismet, Erkmen Aydan M., Matsuno Fumitoshi, Chatterjee Ranajit and Kamegawa Tetsushi, (2002). Snake robots to the rescue! *IEEE Robotics and Automation Magazine*, pp.17-25.

Fjerdingen, S.A, Liljeback, P and Transeth, A. (2009). A snake-like robot for internal inspection of complex pipe structures (PIKo). *In 2009 IEEE/RSJ International Conference on Intelligent Robots and Systems (IROS 2009).* pp. 5665-5671.

Fumitoshi Matsuno and Hiroki Sato, (2005). Trajectory Tracking Control of Snake Robots Based on Dynamic Model. *Proceedings of the 2005 IEEE International Conference on Robotics and Automation Barcelona*, Spain, April 2005. pp 3029 - 3034

G. Granosik,M. G. Hansen, and J. Borenstein, (2005). The Omnitread Serpentine Robot for Industrial Inspection and Surveillance. *Industrial Robot*. 32(2), pp.139–148.

Gonzalez-Gomez, J. (2008). *Modular Robotics and Locomotion: application to limbless robots*. PhD Thesis. Retrieved from http://www.iearobotics.com/downloads/2008-11-08-Tesis-Juan/Thesis_PhD_Juan_Gonzalez_Gomez-2008.pdf (accessed March 2015)

H. Ohno and S. Hirose, (2001). Design of slim slime robot and its gait of locomotion, *In Proc. IEEE/RSJ Int. Conf. Intelligent Robots and Systems*, vol. 2, pp.707–715.

H. Yamada, S. Hirose 2006. Development of Practical 3-Dimensional Active Cord Mechanism ACM-R4, *Robotics and Mechatronics*, 18(3).

Healthy Being, (2014). *The Blessing of the Christchurch Earthquakes*. Retrieved from http://www.healthybeing.co.nz/christchurch_earthquakes.html (accessed April 2014).

Hirose, S. and Fukushima, E.F. (2004). Snakes and strings: new robotic components for rescue operations. *International Journal of Robotics Research*. Vol23, PP341-9..

J. Burdick, J. Radford, and G. Chirikjian, (1993). A 'sidewinding' locomotion gait for hyper-redundant robots. *In Proc. IEEE Int. Conf. Robotics and Automation*, May 1993, pp. 101–106.

J. Casper, (2002). *Human-Robot Interaction during the Robot-Assisted Urban Search and Rescue Response at the World Trade Centre*. MS Thesis, Computer Science and Engineering, USF, 2002.

Kamegawa Tetsushi, Yamasaki Tatsuhiro, Igarashi Hiroki and Matsuno Fumitoshi, (2004). Development of the snake-like rescue robot "KOHGA". *In Proceedings - IEEE International Conference on Robotics and Automation*. April 26, 2004 - May 1, 2004, pp. 5081-5086,.

T. Kane and D. Lecison, (2000). Locomotion of snakes: a mechanical 'explanation'. *International Journal of Solids and Structures*, 37 (41), pp.5829–5837.

Liljebäck, Pål, (2012). *Snake robots: modelling, mechatronics, and control*. New York: Springer, pp.2.

Maruyama, Haruo and Ito, Kazuyuki, (2010). Semi-autonomous snake-like robot for search and rescue. *In 8th IEEE International Workshop on Safety, Security, and Rescue Robotics*, SSRR-2010, July 26, 2010 - July 30, 2010.

Ma, S. (2001). Analysis of creeping locomotion of a snake-like robot. *Advanced Robotics.* 15(2), pp.205-224

Ma, S. and Wu, X. (2010) . CPG-based control of serpentine locomotion of a snake-like robot. *Mechatronics*, 20(2), pp.326-334, ISSN 0957-4158

Mattia F, Paolo A and Luigi F. (2004). *Bio-inspired emergent control of locomotion systems*. World Scientific Publishing.

Mori, M. and Hirose, S. (2001). Development of active cord mechanism ACM-R3 with agile 3D mobility Intelligent Robots and Systems. *In IEEE/RSJ International Conference* . vol.3, 2001, pp.1552 - 1557.

Nataliia Sergiienko and Lei Chen, (2014). Adaptive head stabilisation system for a snake-like robot. *Proceedings of Australasian Conference on Robotics and Automation*. 2-4 Dec 2014.

Paap K.L., T. Christaller, and F. Kirchner, (2000). A robot snake to inspect broken buildings. *InProceeding of the 2000 IEEE/ RSJ International Conferenceon Intelligent Robots and Systems*, pp. 2079–2082.

ROBOTNOR, (2014). *Snake robots*. Retrieved from http://robotnor.no/expertise/robotic-systems/snake-robots/ (accessed April 2014).

Sh. Hasanzadeh and A. Akbarzadeh Tootoonchi, (2008). Obstacle avoidance of snake robot moving with a novel gait using two-level PID controller. *In 2008 IEEE International Conference on Robotics, Automation and Mechatronics*, September 21, 2008 - September 24, 2008, pp.427-432.

S. Hirose, (1993). *Biologically Inspired Robots: Snake-Like Locomotors and Manipulators*. Oxford: Oxford University Press.

S. Ma, Y. Ohmameuda, and K. Inoue, (2004). Dynamic analysis of 3-dimensional snake robots. *in Proc. IEEE/RSJ Int. Conf. On Intelligent Robots and Systems*, pp. 767–772.

National Science Foundation. (2015). *Snake Locomotion*. Retrieved from https://www.youtube.com/watch?v=5CchyctRFrQ (accessed March 2015).

Snake Robots. (2014). *Snake Robots*. Retrieved from http://www.snakerobots.com/index.html (accessed April 2014).

Wang Yang, Li Bin, Chen Li and Lin Chen, (2003). Design and realization of snake-like robot control system[j]. *Robot*, 25(6), pp.491-494,500.

Wikipedia, (2014).2011. *Christchurch earthquake*. Retrieved from http://en.wikipedia.org/wiki/Christchurch_earthquake (accessed April 2014).

Wikipedia, (2014). *Earthquakes in New Zealand*. Retrieved from http://en.wikipedia.org/wiki/Earthquakes_in_New_Zealand (accessed April 2014)

Williamson MM. (1998). Rhythmic robot arm control using oscillators. *In: Proceedings of 1998 international conference on intelligent robots and systems*, Victoria, Canada, 1998. pp.77–83.

Z. Y. Bayraktaroglu, A. Kilicarslan, A. Kazucu, V. Hugel and P. Blazevic, (2006). Design and control of biologically inspired wheel-less snake-like robot. *In: Proc. IEEE/RAS-EMBS Int. Conf. Biomedical Robotics and Biomechatronics*. pp. 1001-1006.

Appendix A

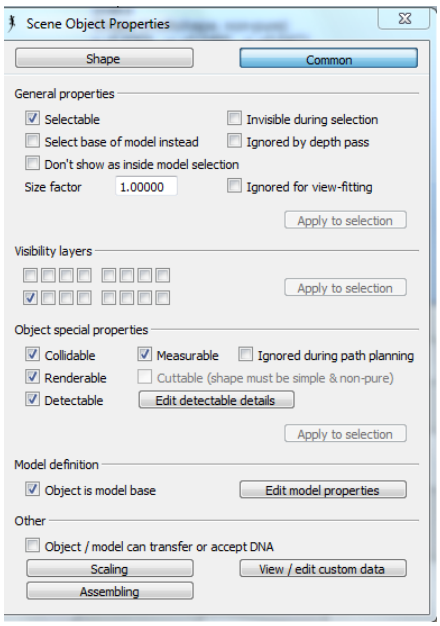

Figure A.1 Common settings of the base respondable object

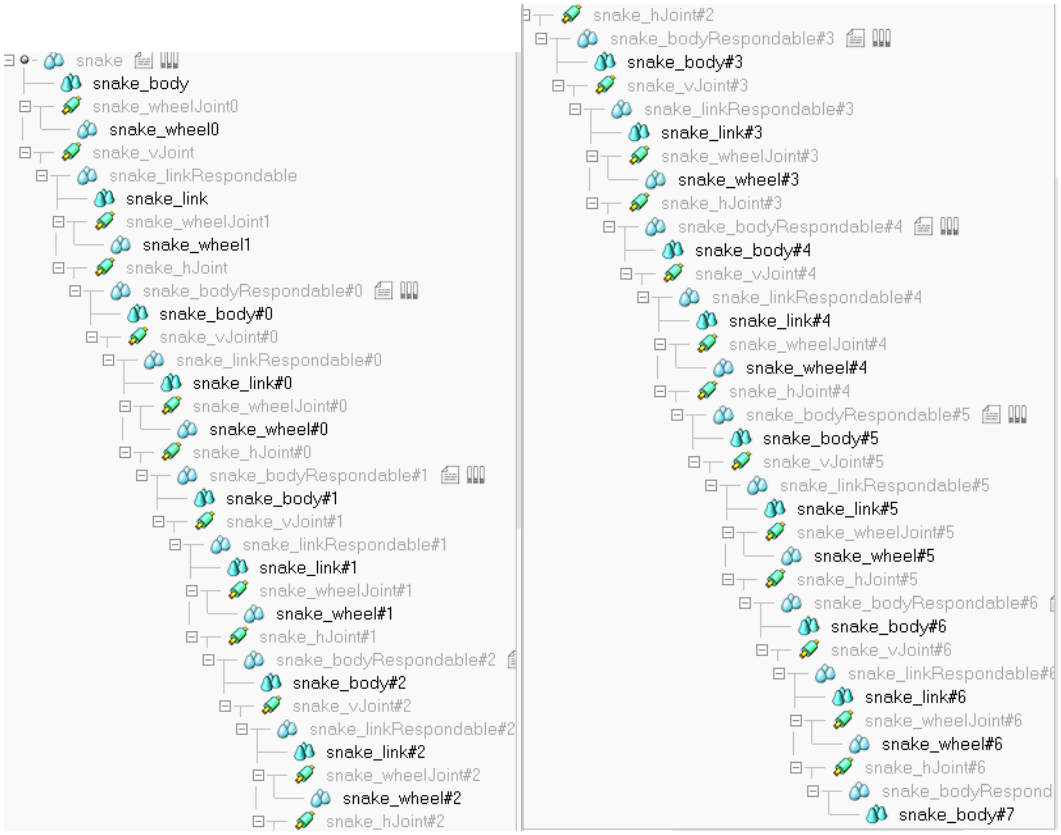

Figure A.2 The configuration of snake robot

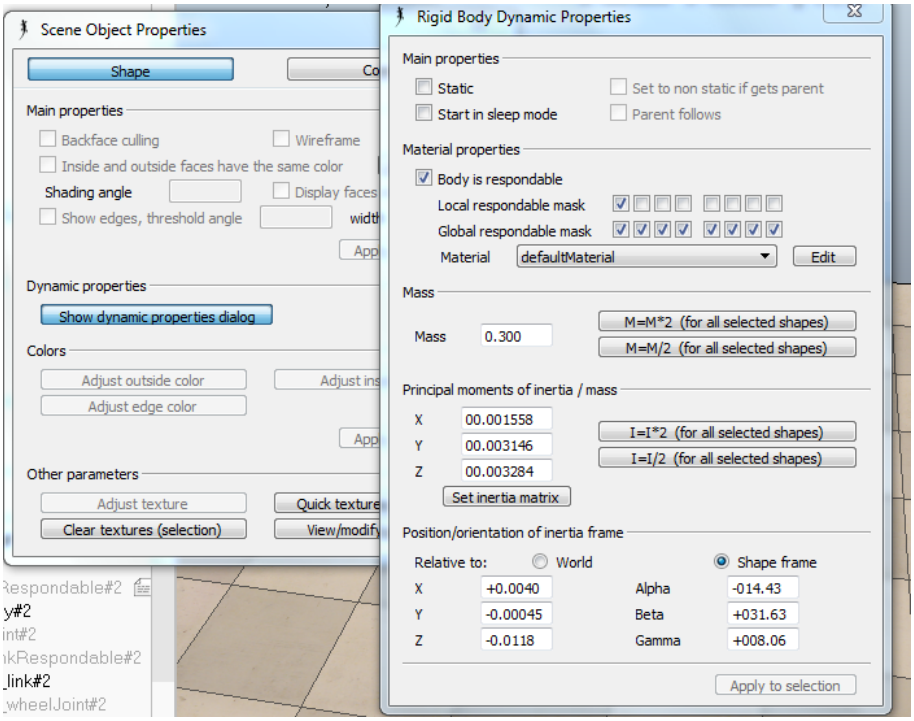

Figure A.3 Dynamic properties of snake body respondable

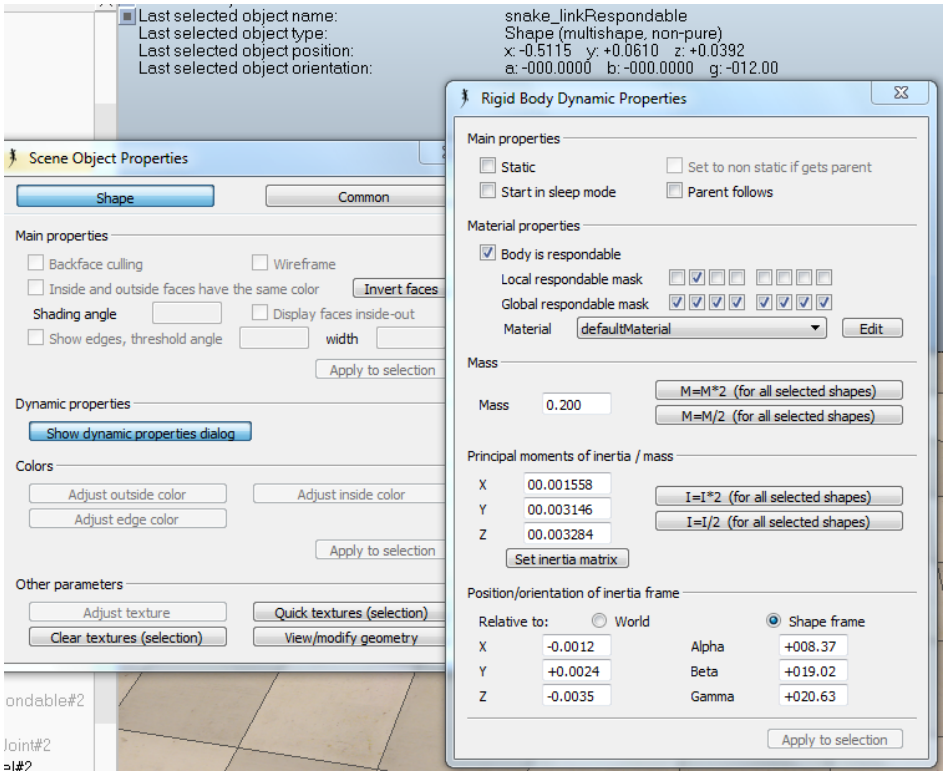

Figure A.4 Dynamic properties of snake link respondable

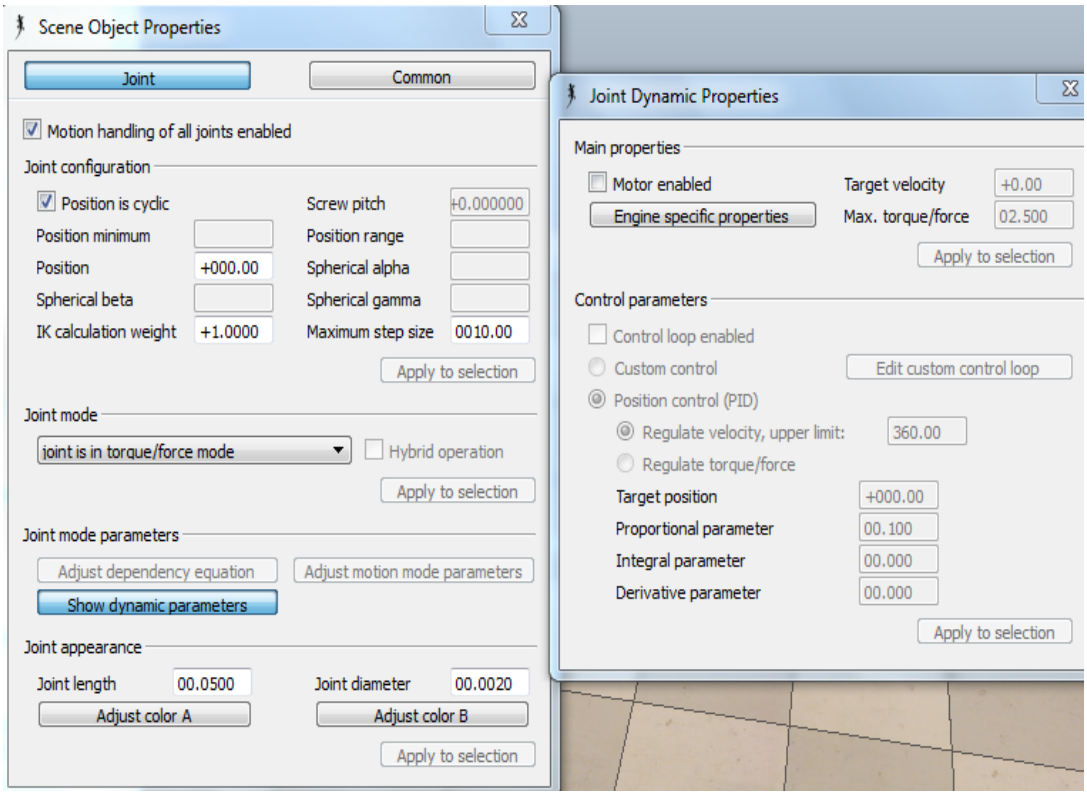

Figure A.5 Dynamic properties of snake wheel joint

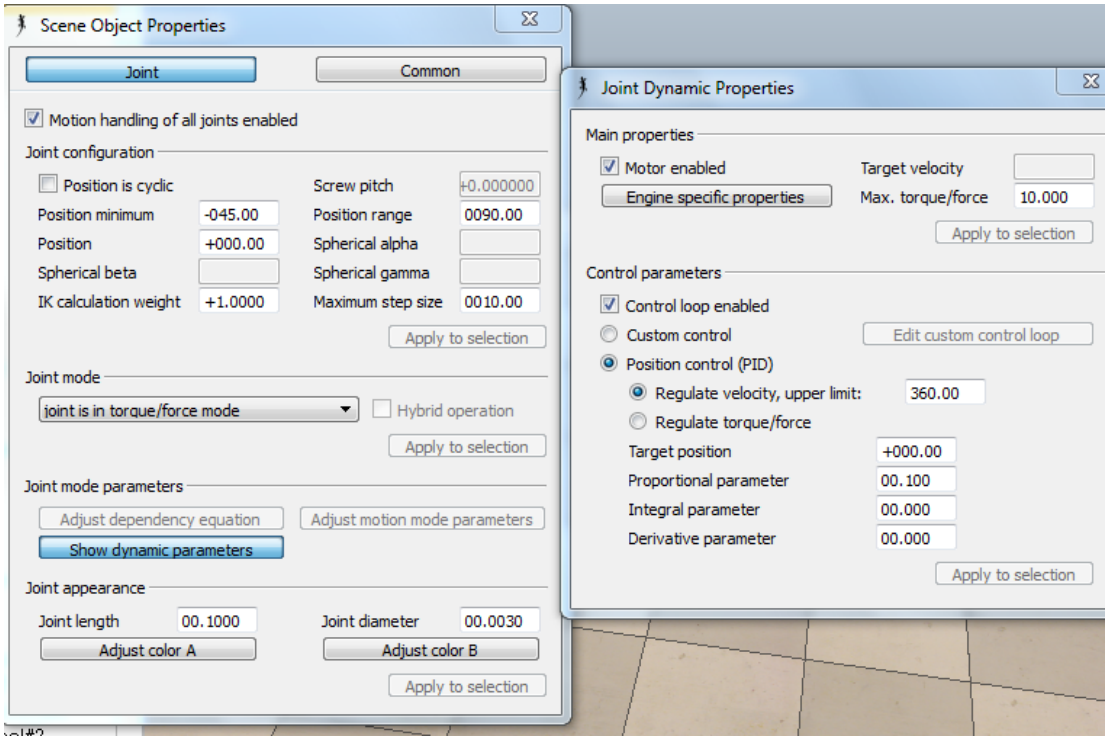

Figure A.6 Dynamic properties of snake vertical joint and horizonal joint

Appendix B

```
==================== analog joysticks ====================
     Case Else
         ps.GetLXYPos(lx,ly)
         ps.GetRXYPos(rx,ry)
         If ry > 0 Then
            index = index + 1
         Elseif ry < 0 Then
            ry = -ry
            index = index - 1
         End If

         If ry = 0 Then
            stop = 1
         Else
            stop = 0
               regy = ry
               actionspeed = 500 - regy * 3
            End If

      devi = lx

    t = actionspeed*index

      If stop=0 Then
           ang0 = 1500+300*Sin((-(pi*1.25)*t)*0.001)-219*Cos((-(pi*1.25)*t)*0.001+8.28*2*(pi/9))
           ang1 = 1500+300*Sin((-(pi*1.25)*t)*0.001+1*2*(pi/9))
           ang2 = 1500+300*Sin((-(pi*1.25)*t)*0.001+2*2*(pi/9))
           ang3 = 1500+300*Sin((-(pi*1.25)*t)*0.001+3*2*(pi/9))
           ang4 = 1500+300*Sin((-(pi*1.25)*t)*0.001+4*2*(pi/9))
           ang5 = 1500+300*Sin((-(pi*1.25)*t)*0.001+5*2*(pi/9))
           ang6 = 1500+300*Sin((-(pi*1.25)*t)*0.001+6*2*(pi/9))
           ang7 = 1500+300*Sin((-(pi*1.25)*t)*0.001+7*2*(pi/9))



           MySer1.SetPosTime(0,ang0+2*devi,actionspeed)
           MySer1.SetPosTime(1,ang1+2*devi,actionspeed)
           MySer1.SetPosTime(2,ang2+2*devi,actionspeed)
           MySer1.SetPosTime(3,ang3+2*devi,actionspeed)
           MySer1.SetPosTime(4,ang4+2*devi,actionspeed)
           MySer1.SetPosTime(5,ang5+2*devi,actionspeed)
           MySer1.SetPosTime(6,ang6+2*devi,actionspeed)
           MySer1.SetPosTime(7,ang7+2*devi,actionspeed)

         For i=8 To 15
            MySer1.SetPosTime(i,1500,actionspeed)
         Next i
```

Figure B.1 The main controlling code in the microcontroller